

1 **Supplementary Material**

3 **Catalyst-free solid-state cross-linking of covalent organic frameworks in confined
4 space**

6 **Dan Wen^{1,3}, Saikat Das², Yu Zhao^{1,2,3,*}, Jingru Fu^{1,2,3}, Zelong Qiao⁴, Yijing Gao^{1,3},**
7 **Yuxia Wang², Ziqiang Zhao², Dapeng Cao⁴, Daoling Peng⁵, Weidong Zhu^{1,3}, Teng**
8 **Ben^{1,2,3,*}**

10 ¹Zhejiang Engineering Laboratory for Green Syntheses and Applications of
11 Fluorine-Containing Specialty Chemicals, Institute of Advanced Fluorine-Containing
12 Materials, Zhejiang Normal University, Jinhua 321004, Zhejiang, China.

13 ²Department of Chemistry, Jilin University, Changchun 130012, Jilin, China.

14 ³Key Laboratory of the Ministry of Education for Advanced Catalysis Materials,
15 Institute of Physical Chemistry, Zhejiang Normal University, Jinhua 321004, Zhejiang,
16 China.

17 ⁴State Key Laboratory of Organic-Inorganic Composites, Beijing University of
18 Chemical Technology, Beijing 100029, China.

19 ⁵Key Laboratory of Theoretical Chemistry of Environment, Ministry of Education,
20 School of Environment, South China Normal University, Guangzhou 510006,
21 Guangdong, China.

23 ***Correspondence to:** Dr. Yu Zhao, Prof. Teng Ben, Zhejiang Engineering Laboratory
24 for Green Syntheses and Applications of Fluorine-Containing Specialty Chemicals,
25 Institute of Advanced Fluorine-Containing Materials, Zhejiang Normal University, 688
26 Yingbin Road, Jinhua 321004, Zhejiang, China. E-mail: zhaoyu@zjnu.edu.cn;
27 tengben@zjnu.edu.cn

28



29 Table of Contents

30	Section S1. Materials and Characterizations	3
31	Section S2. Synthetic Procedures	6
32	Section S3. Fourier-transform infrared spectroscopy	9
33	Section S4. Solid-state ^{13}C NMR spectra	12
34	Section S5. Acid-digested CPOF-4-265 °C-84 h	13
35	Section S6. X-ray photoelectron spectroscopy	21
36	Section S7. Electron paramagnetic resonance	24
37	Section S8. UV-visible spectra	26
38	Section S9. Density Functional Theory Calculations	27
39	Section S10. Synthesis of polymer-model	28
40	Section S11. PXRD patterns and structures	32
41	Section S12. Nitrogen adsorption	39
42	Section S13. SEM image	48
43	Section S14. TEM image	49
44	Section S15. TGA curves	51
45	Section S16. Chemical stability tests	52
46	Section S17. Reaction kinetics and thermodynamic studies	54
47	Section S18. Electrical conductivity measurements	57
48	Section S19. Unit cell parameters and fractional atomic coordinates	58
49	Section S20. References	87
50		

51 **Section S1. Materials and Characterizations**

52 **S1.1. Materials**

53 All chemicals and solvents were purchased from commercial suppliers.

54 4,4'-diaminobiphenyl (DABP) and 4,4"-diamino-p-terphenyl (DATP) were purchased
55 from Aladdin®. 1,2-dichlorobenzene (*o*-DCB), *N,N*-dimethylacetamide (DMAc) and
56 diphenyl sulfone were obtained from J&K scientific LTD. Acetic acid and organic
57 solvents including dichloromethane (DCM), *n*-hexane, acetone and tetrahydrofuran
58 (THF) were purchased from Xilong Scientific.

59 1,3,5-tri(4-formylphenylethynyl)benzene (TFPEB) was synthesized. All reagents and
60 solvents were used without further purification unless otherwise specified.

61

62 **S1.2. Characterizations**

63 ***Nuclear magnetic resonance (NMR) spectroscopy.*** ^1H NMR spectra were measured on
64 a Bruker Fourier 400 MHz spectrometer. Solid-state NMR spectra were recorded at
65 ambient pressure on a Bruker Fourier 600 MHz spectrometer using a standard CP pulse
66 sequence probe with 3.2 mm (outside diameter) zirconia rotors.

67

68 ***Fourier transform infrared (FT-IR) spectroscopy.*** The FT-IR spectra (KBr) were
69 obtained using a SHIMADZU IRAffinity-1 Fourier transform infrared
70 spectrophotometer. A SHIMADZU UV-2450 spectrophotometer was used for all
71 absorbance measurements.

72

73 ***Powder X-ray diffraction (PXRD) analysis.*** Powder X-ray diffraction (PXRD) patterns
74 were carried out in reflection mode on a Bruker D8 advance powder diffractometer
75 with Cu K α ($\lambda = 1.5418 \text{ \AA}$) line focused radiation at 40 kV and 40 mA from $2^\circ = 1.0^\circ$
76 up to 40° with 0.020481 increment by Bragg-Brentano. The powdered sample was
77 added to the glass and compacted for measurement.

78

79 ***Thermogravimetric analysis (TGA).*** Thermogravimetric analysis (TGA) was recorded
80 on a SHIMADZU DTG-60 thermal analyzer under N₂. The operational range of the
81 instrument was from 30 to 800 °C at a heating rate of 10 °C min⁻¹ with N₂ flow rate of
82 30 mL min⁻¹.

83

84 **Raman spectroscopy characterization.** Raman spectra were recorded on a Renishaw
85 inVia-Reflex confocal Raman microscope with an excitation wavelength of 325 nm.
86

87 **X-ray photoelectron spectroscopy (XPS).** XPS was obtained on an ESCALAB 250
88 spectrophotometer with Al-K α radiation. The binding energy (BE) values were referred
89 to the C single bond (C, H) contribution of the C 1s peak fixed at 284.8 eV.
90

91 **Atomic force microscope (AFM).** AFM images were obtained by testing with German
92 Bruker Dimension 3100 instrument in tapping mode.
93

94 **Electron paramagnetic resonance (EPR).** EPR spectra are recorded on a Bruker
95 EMXplus-10/12 spectrometer under room temperature. The microwave frequency was
96 9.8 GHz and the modulation amplitude microwave power was about 2 mW.
97

98 **Nitrogen isotherm measurements.** Nitrogen sorption experiments were performed at
99 77 K up to 1 bar using a nanometric sorption analyzer. The adsorption–desorption
100 isotherms of N₂ were obtained at 77 K using a BELSORP MAX gas sorption analyzer.
101 Before sorption analysis, the sample was evacuated at 100 °C for 12 h using a
102 turbomolecular vacuum pump. Specific surface areas were calculated from nitrogen
103 adsorption data by multipoint BET analysis. Quenched solid density functional theory
104 (QS-DFT) was applied to analyze the N₂ isotherm based on the model of N₂@77 K on
105 carbon with cylindrical pores.
106

107 **Scanning electron microscopy (SEM).** Scanning electron microscopy (SEM) was
108 performed on a Zeiss Gemini SEM 300 microscope instrument. Samples were prepared
109 by dispersing the material onto conductive adhesive tapes attached to a flat aluminum
110 sample holder and then coated with gold.
111

112 **Transmission electron microscope (TEM).** High resolution transmission electron
113 microscope (HR-TEM) analysis was collected on a JEOL JEM-2100 microscope
114 instrument at 200 kV. synthesized sample was dispersed into ethyl alcohol to obtain a
115 highly dispersed suspension. Then, one droplet was transferred onto a carbon film
116 supported TEM grid.

117 **Electrical conductivity measurements.** Electrochemistry experiments were conducted
118 on a CHI660C Electrochemical Workstation (Shanghai ChenHua Electrochemical
119 Instrument). The obtained powder was grinded before adding into a 0.5-cm die. Then
120 the pressure of die was slowly increased to 4.0 MPa and kept for 1 hours to prepared
121 pellets (diameter = 0.5 cm, thickness = 0.5 cm). Two pieces of gold (diameter = 0.5 cm)
122 with wires are attached to both sides of the pellet. The current-voltage (I-V)
123 measurement was performed in conditions by sweeping the voltage from -1.0 V to 1.0
124 V. The obtained conductivity was collected at 25 °C in N₂ atmosphere.
125

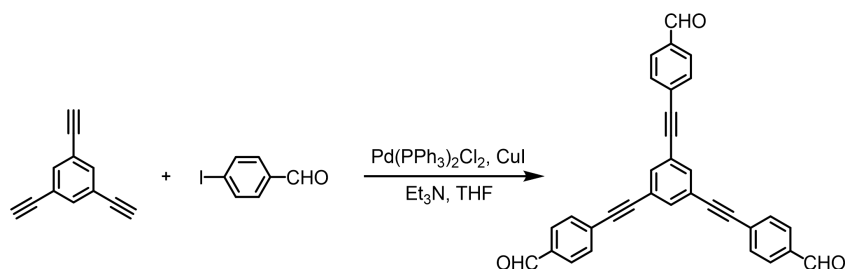
126 **Density Functional Theory Calculations.** frontier orbital calculations were performed
127 at the Generalized gradient approximation (GGA) level in the form of
128 Perdew-Burke-Ernzerhoff (PBE),^[1] using the Dmol3 module in Materials Studio
129 version 8.0². The convergence criterion of 10⁻⁶ eV with max to 50 cycles was used for
130 self-consistent field (SCF).

131

132 **Section S2. Synthetic Procedures**

133 Synthesis of 1,3,5-tri(4-formylphenylethynyl)benzene (TFPEB).

134



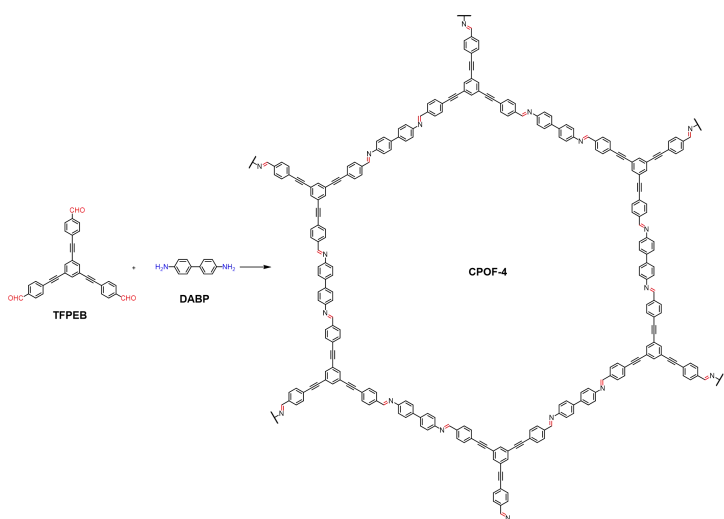
135

136

137 Under a nitrogen atmosphere, 1,3,5-triethynylbenzene (1.2 g, 8.0 mmol, 1.0 eq.),
 138 4-iodobenzaldehyde (5.6 g, 24.0 mmol, 3.0 eq.),
 139 dichlorobis(triphenylphosphine)palladium(II) (0.34 g, 0.48 mmol, 0.02 eq.) were
 140 dissolved in 200 mL of anhydrous THF, Dry triethylamine (8.0 mL, 57 mmol) was
 141 added and the mixture stirred for 10 mins, then the catalyst copper(I) iodide (0.19 g, 1.0
 142 mmol, 0.04 eq.) was added, turning the solution to dark brown. After stirring for 16 h at
 143 room temperature, the solvent was evaporated at reduced pressure and the mixture was
 144 washed with brine saturated solution of NH₄Cl and extracted with DCM. The
 145 purification was made by column chromatography on silica gel using dichloromethane
 146 as eluent to afford the desired product as a colorless solid (2.18 g, Yield: 59%); ¹H
 147 NMR (400 MHz, CDCl₃): δ_H 10.04 (s, 3H), 7.90 (d, *J* = 8.3 Hz, 6H), 7.74 (s, 3H), 7.69
 148 (d, *J* = 8.2 Hz, 6H); ¹³C NMR (101 MHz, CDCl₃): δ_C 191.5, 136.0, 135.0, 132.4, 129.8,
 149 128.9, 123.8, 91.3, 90.1.

150

151 Preparation of CPOF-4

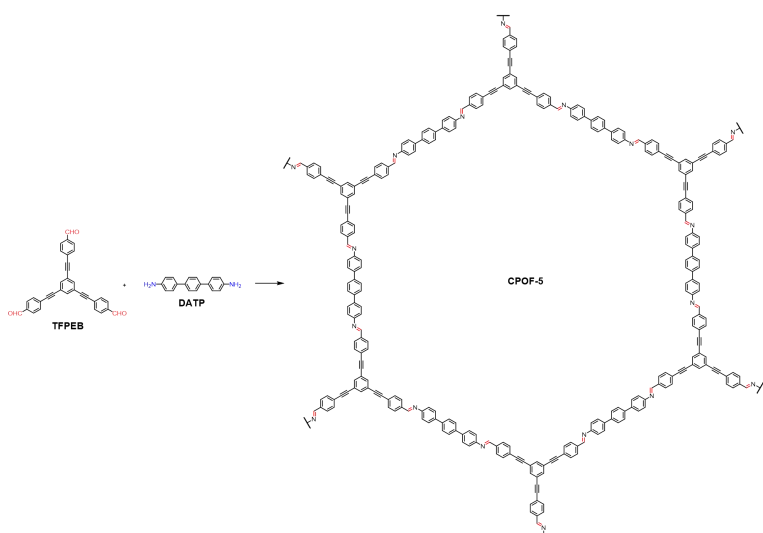


152

153 A Pyrex tube measuring o.d. × i.d. = 10 × 8 mm² was charged with
 154 1,3,5-Tri(4-formylphenylethynyl)benzene (TFPEB, 13.9 mg, 0.03 mmol),
 155 4,4'-diaminobiphenyl (DABP, 8.3 mg, 0.045 mmol) in a mixed solution of
 156 o-dichlorobenzene (0.5 mL), dimethylacetamide (0.5 mL) and 6.0 M acetic acid (0.1
 157 mL). The Pyrex tube was flash frozen in a liquid nitrogen bath sealed under vacuum.
 158 Upon warming to room temperature, the tube was placed in an oven at 120 °C for three
 159 days. The yellow solid was isolated by filtration and washed with THF (3 × 15 mL),
 160 acetone (3 × 15 mL) and *n*-hexane (3 × 15 mL). The powder was dried at 80 °C under
 161 vacuum overnight to afford the CPOF-4 as a yellow crystalline solid (15.4 mg, Yield:
 162 75%).

163

164 Preparation of CPOF-5

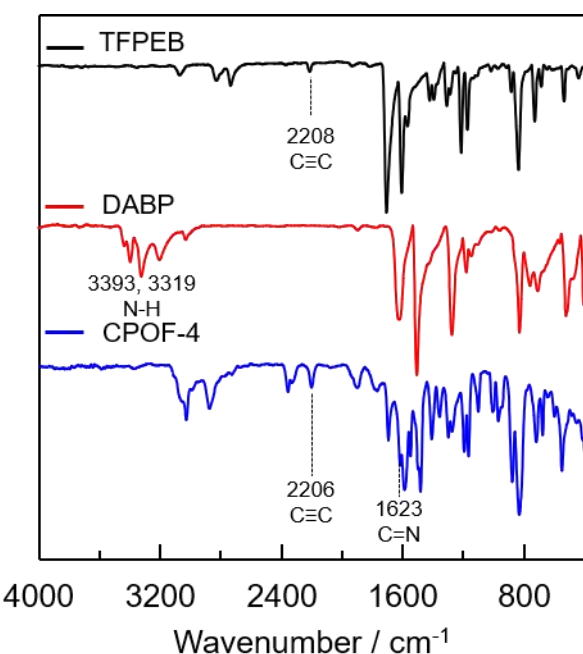


165

166 A Pyrex tube measuring o.d. × i.d. = 10 × 8 mm² was charged with
 167 1,3,5-Tri(4-formylphenylethynyl)benzene (TFPEB, 13.9 mg, 0.03 mmol),
 168 4,4"-diamino-*p*-terphenyl (DATP, 11.7 mg, 0.045 mmol) in a mixed solution of
 169 *o*-dichlorobenzene (0.5 mL), dimethylacetamide (0.5 mL) and 6.0 M acetic acid (0.1
 170 mL). The Pyrex tube was flash frozen in a liquid nitrogen bath sealed under vacuum.
 171 Upon warming to room temperature, the tube was placed in an oven at 120 °C for three
 172 days. The yellow solid was isolated by filtration and washed with THF (3 × 15 mL),
 173 acetone (3 × 15 mL) and *n*-hexane (3 × 15 mL). The powder was dried at 80 °C under
 174 vacuum overnight to afford the CPOF-5 as a yellow crystalline solid (17.1 mg, Yield:
 175 71%).

176

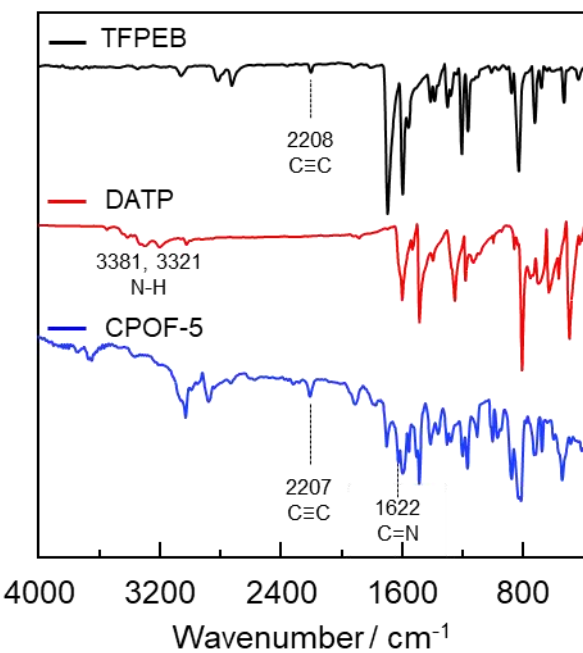
177 **Synthesis and activation of CL-COFs.** For example, a 5 mL vial charged with
 178 CPOF-4 (100.0 mg) and diphenyl sulfone (3 g), The vial was then transferred to a
 179 tubular furnace and evacuated-filled with N₂ by five cycles. subsequently, the
 180 temperature was raised to 265 °C at the rate of 10 °C/min in N₂ flowing atmosphere
 181 with the flow rate of 20 mL/min. After heating at 265 °C for a certain period of time,
 182 the temperature was reduced to room temperature at the rate of 10 °C/min. Finally, the
 183 obtained product was washed with THF and acetone to remove the residual diphenyl
 184 sulfone, dried at 120 °C under vacuum over-night to afford the CPOF-4-265 °C-*X* h (*X*=
 185 12, 48 and 84) as a brown black crystalline solid. Similarly, the thermally cross-linked
 186 products of CPOF-5 are named CPOF-5-265 °C-*X* h (*X*= 48 and 84).

187 **Section S3. Fourier-transform infrared spectroscopy**

188

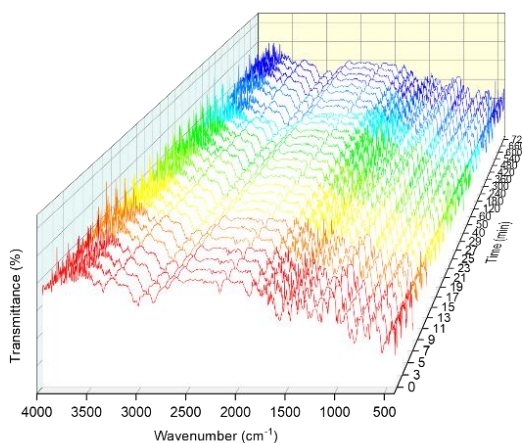
189 **Supplementary Figure 1.** FT-IR spectra of CPOF-4 (blue), DABP (red), TFPEB
190 (black).

191



192

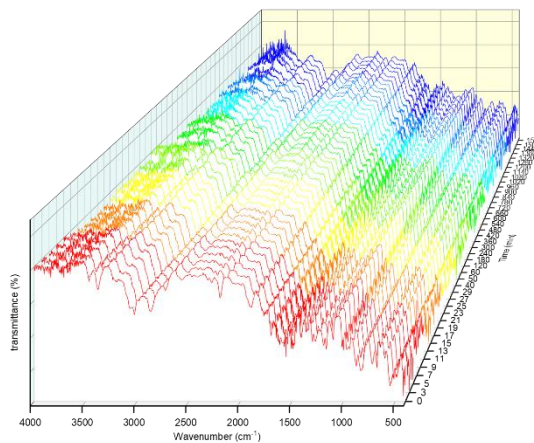
193 **Supplementary Figure 2.** FT-IR spectra of CPOF-5 (blue), DATP (red), TFPEB
194 (black).



195

196 **Supplementary Figure 3.** In-situ variable temperature FT-IR of CPOF-4 at 215 °C.

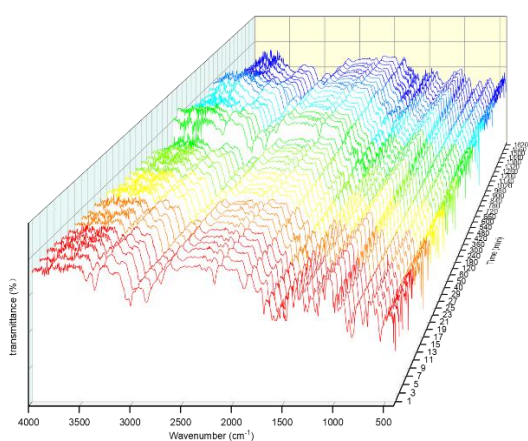
197



198

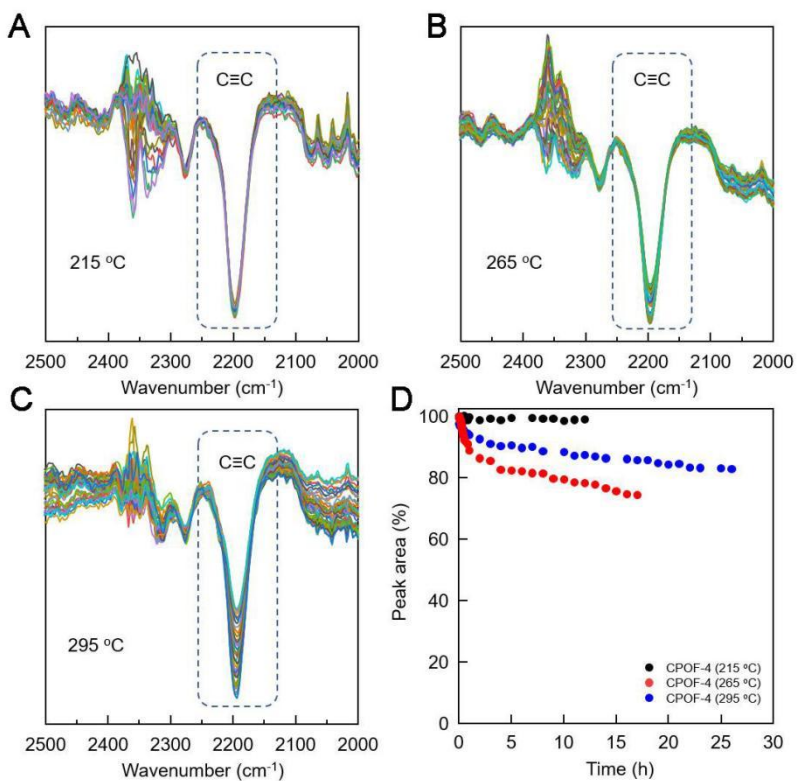
199 **Supplementary Figure 4.** In-situ variable temperature FT-IR of CPOF-4 at 265 °C.

200



201

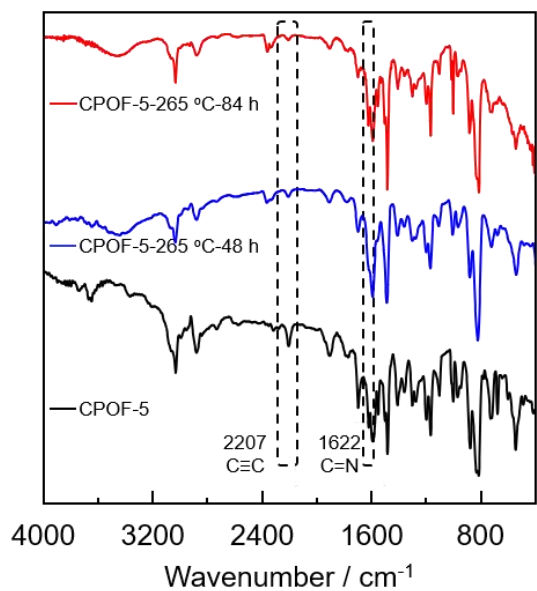
202 **Supplementary Figure 5.** In-situ variable temperature FT-IR of CPOF-4 at 295 °C.



203

204 **Supplementary Figure 6.** (A-C) *In-situ* variable temperature FT-IR of CPOF-4 at 215
 205 °C, 265 °C and 295 °C respectively; (D) Temperature induced variations in the peak
 206 area of C≡C stretching.

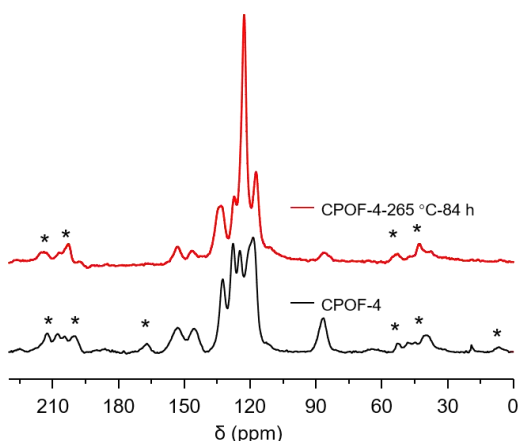
207



208

209 **Supplementary Figure 7.** FT-IR spectra analyses of CPOF-5 compared with the
 210 CPOF-5-265 °C-48 h and CPOF-5-265 °C-84 h.

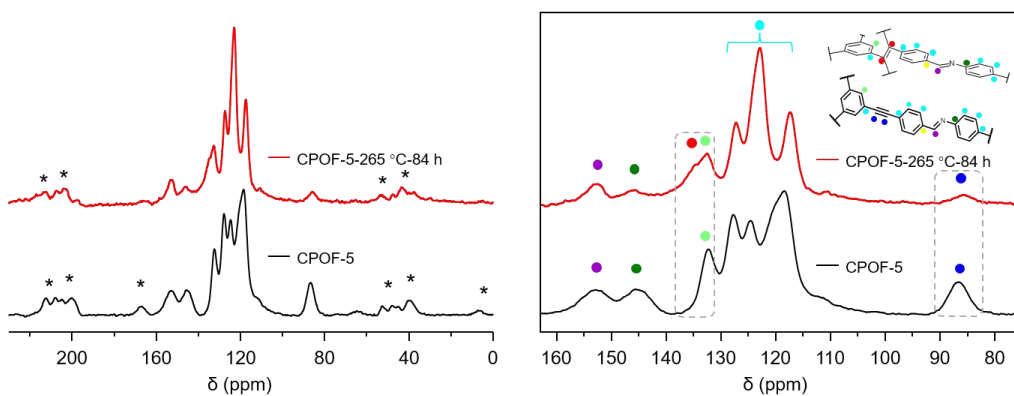
211 **Section S4. Solid-state ^{13}C NMR spectra**



212

213 **Supplementary Figure 8.** ^{13}C CP-MAS NMR spectra of CPOF-4 and CPOF-4-265
214 °C-84 h.

215



216

217 **Supplementary Figure 9.** ^{13}C CP-MAS NMR spectra of CPOF-5 and CPOF-5-265
218 °C-84 h.

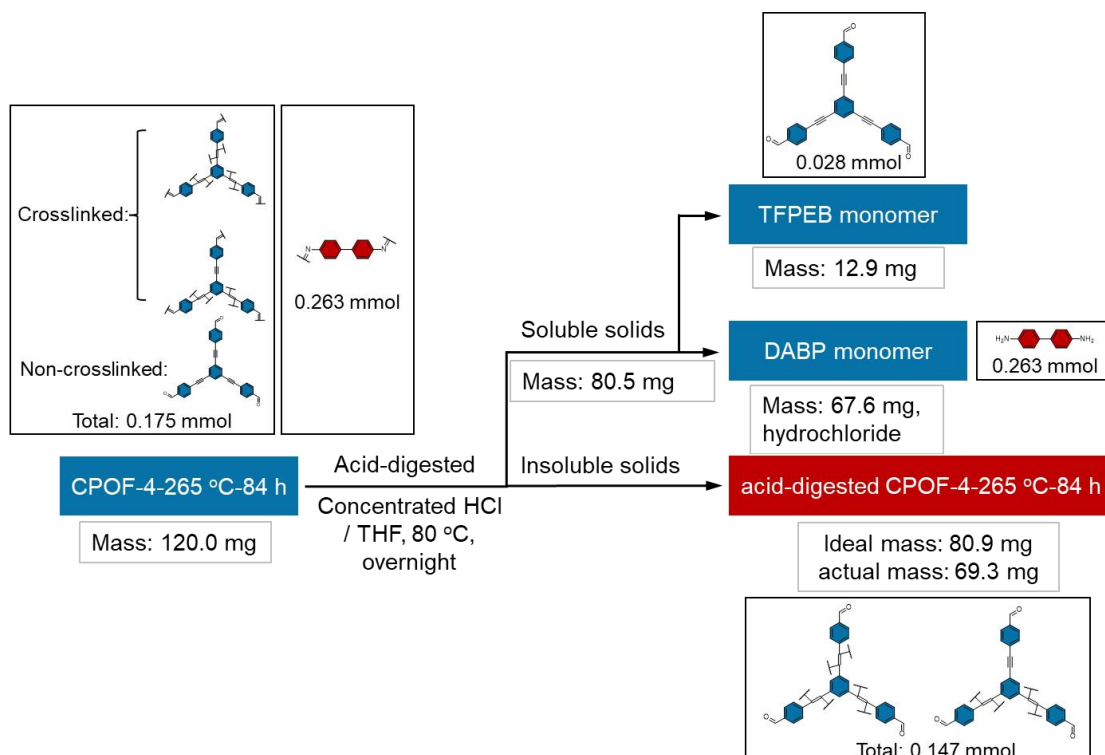
219 **Section S5. Acid-digested CPOF-4-265 °C-84 h**

220 Since the conversion rate of the acetylenic groups in COFs was not particularly high, a
221 small fraction of the original COF remained in the products, posing interference to the
222 analysis and characterization of polyacetylene. Fortunately, the reversible imine bonds
223 could be easily broken under acidic conditions. Thus, the acid hydrolysis experiment on
224 CPOF-4-265 °C-84 h effectively removed the non-crosslinked residues (soluble
225 fraction) from the reaction, while preserving the formed polyacetylene chain structures
226 (insoluble fraction). This approach facilitated the direct characterization of
227 polyacetylene formation.

228

229 The activated CPOF-4-265 °C-84 h (120 mg), concentrated hydrochloric acid (5.0 mL)
230 and THF (15.0 mL) were added into a flask. The mixture was heated at 80 °C for
231 overnight under nitrogen atmosphere. After cooling to room temperature, the insoluble
232 solid was isolated by filtration and washed with deionized water, MeOH, THF and
233 dried at 80 °C under vacuum overnight. The collected filtrate was rotary evaporated to
234 remove all solvents and used for subsequent characterization analysis.

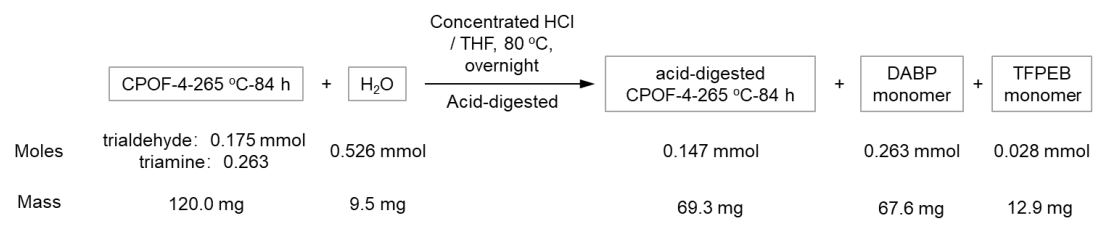
235 As depicted in Supplementary Figure 10, CPOF-4-265 °C-84 h comprised crosslinked
236 and non-crosslinked segments. Following acid hydrolysis, the non-crosslinked
237 segments were soluble in organic solvents, and characterization of the resulting soluble
238 solid was achieved through ¹H-NMR spectroscopy after solvent removal. Additionally,
239 since biphenylamine, uninvolved in the crosslinking reaction, is fully released upon
240 hydrolysis, thus, the soluble TFPEB monomer can be quantified through ¹H-NMR. The
241 measured weight of the insoluble solid obtained after acid hydrolysis was 69.3 mg,
242 which was lower than the theoretical mass (assuming complete crosslinking of the
243 acetylenic groups). This discrepancy can be primarily attributed to the presence of a
244 small amount of soluble TFPEB monomer in the hydrolysis products. Additionally,
245 precise weighing of the products obtained during the hydrolysis reaction indicated that
246 the process adhered to the principle of mass conservation.



247

248 **Supplementary Figure 10.** Schematic diagram of hydrolysate analysis process.

249

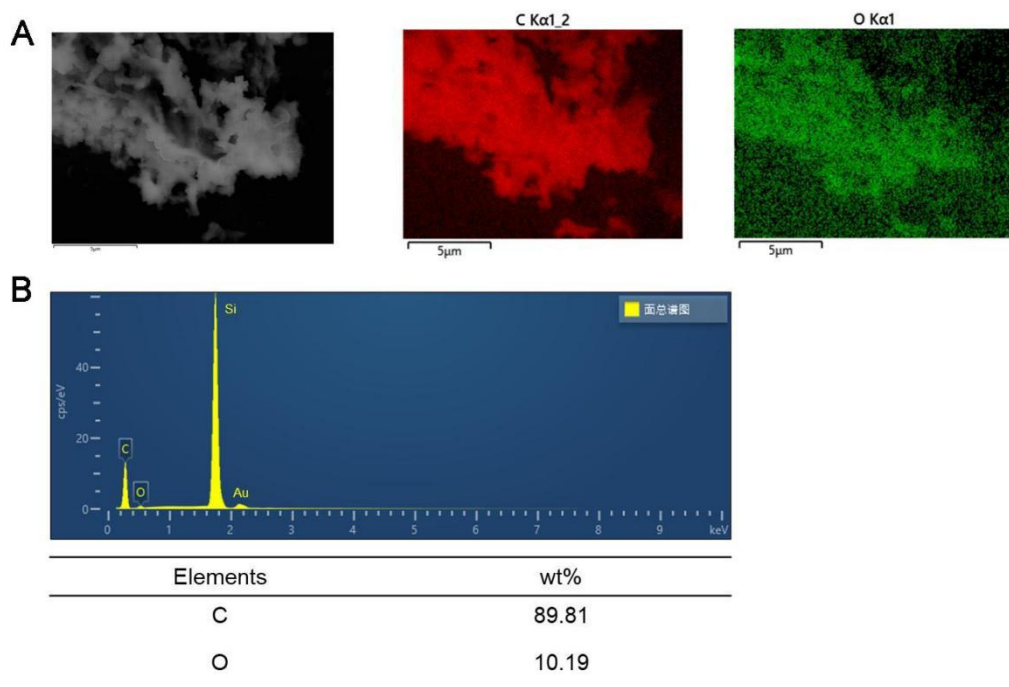


250

251 **Supplementary Figure 11.** The hydrolysis reaction equation of CPOF-4-265 °C-84 h.

252

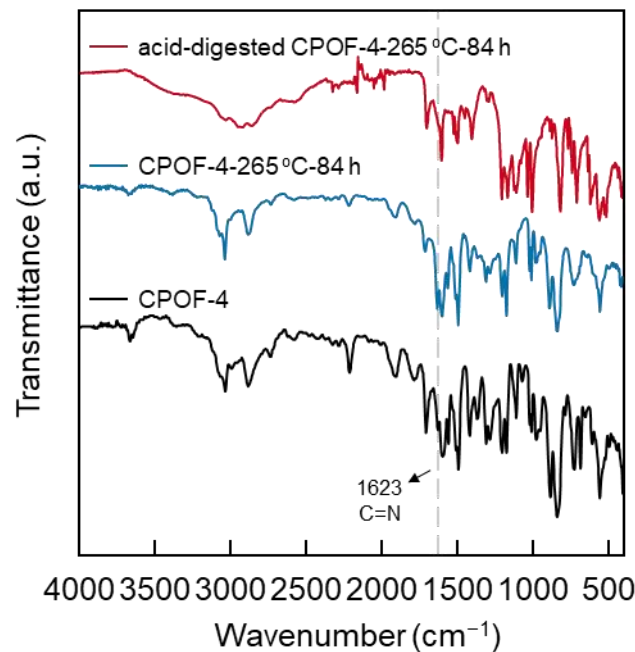
253



254

255 **Supplementary Figure 12.** (A) SEM mapping images of elements C and O in
 256 acid-digested CPOF-4-265 °C-84 h; (B) EDS elementals content analysis from
 257 SEM-related EDS in acid-digested CPOF-4-265 °C-84 h.

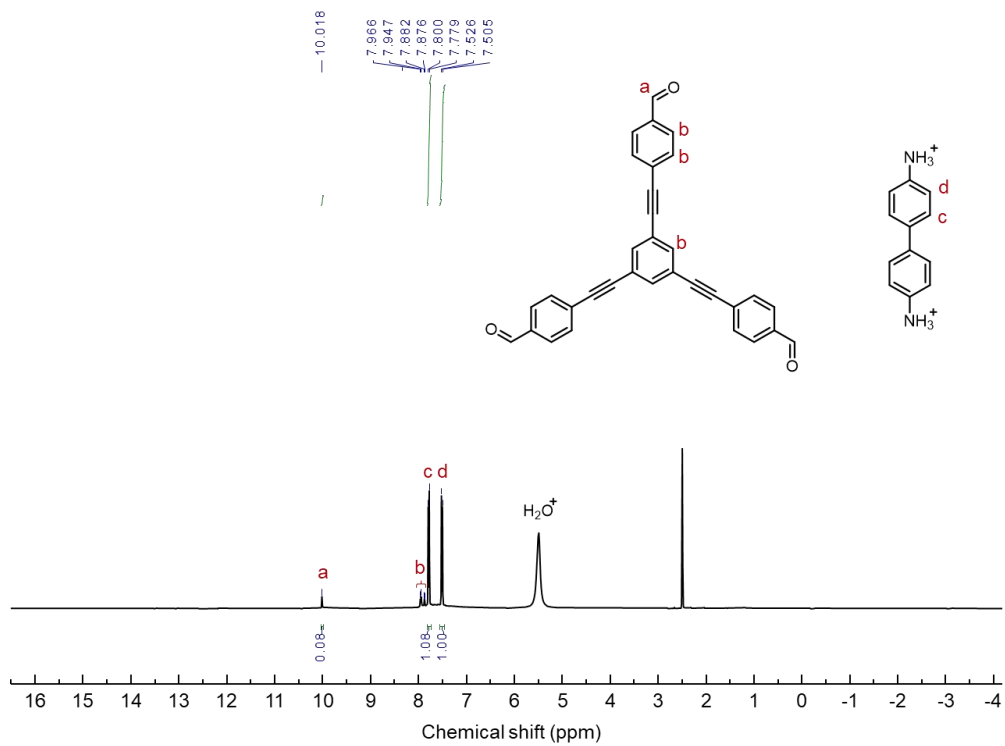
258



259

260 **Supplementary Figure 13.** FT-IR spectra of CPOF-4 (black), CPOF-4-265 °C-84 h
 261 (dark blue), and acid-digested CPOF-4-265 °C-84 h (red), the characteristic peak of
 262 imine bond disappeared after hydrolysis.

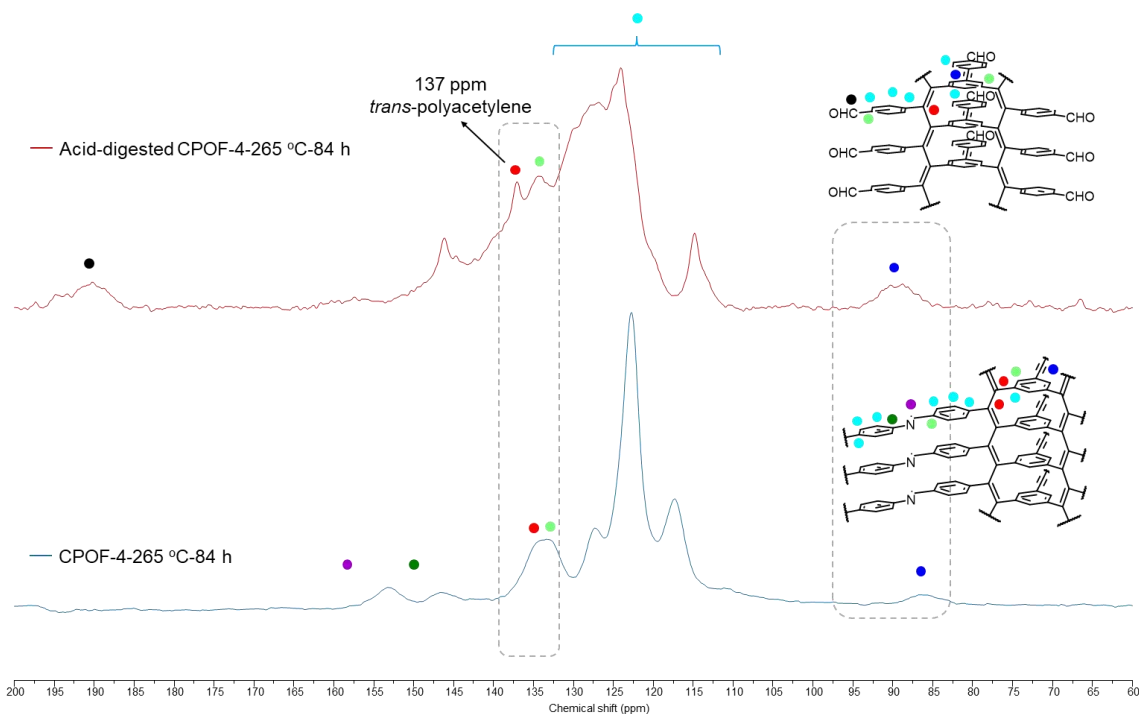
263



264

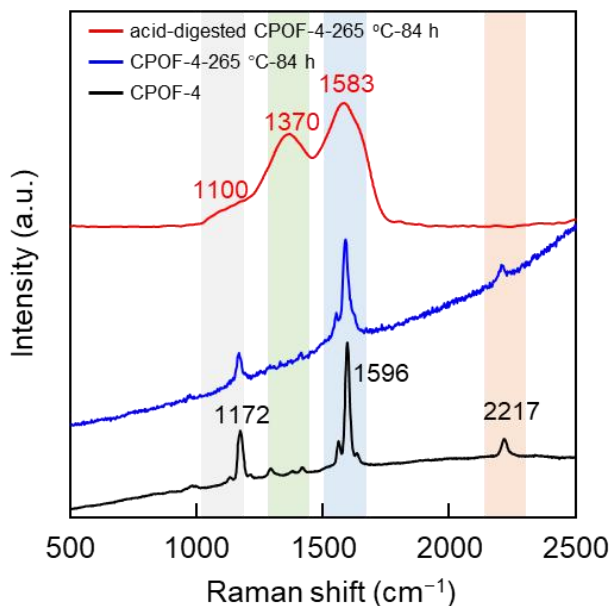
265 **Supplementary Figure 14.** The ^1H NMR spectra of soluble solids.

266



267

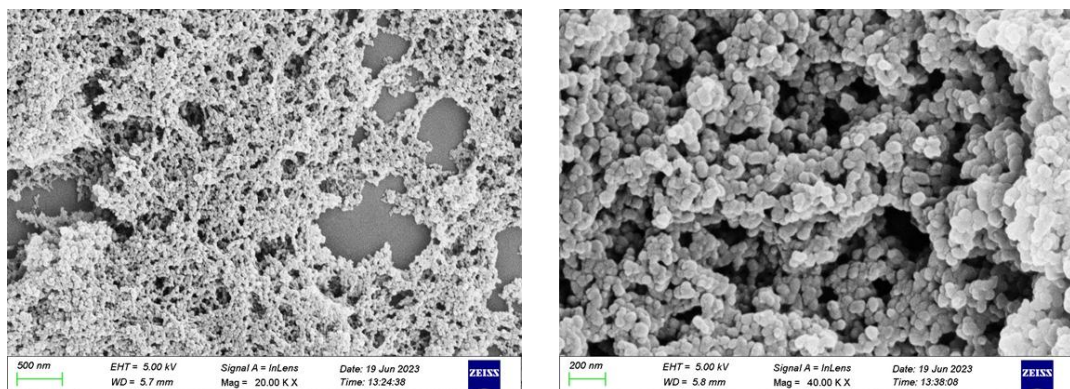
268 **Supplementary Figure 15.** ^{13}C CP-MAS NMR spectra of CPOF-4-265 °C-84 h and
269 acid-digested CPOF-4-265 °C-84 h



270

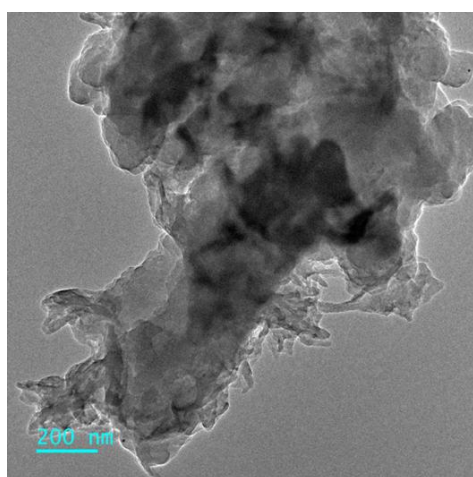
271 **Supplementary Figure 16.** Raman spectra of CPOF-4 (black), CPOF-4-265 °C-84 h
272 (blue) and acid-digested CPOF-4-265 °C-84 h (red).

273

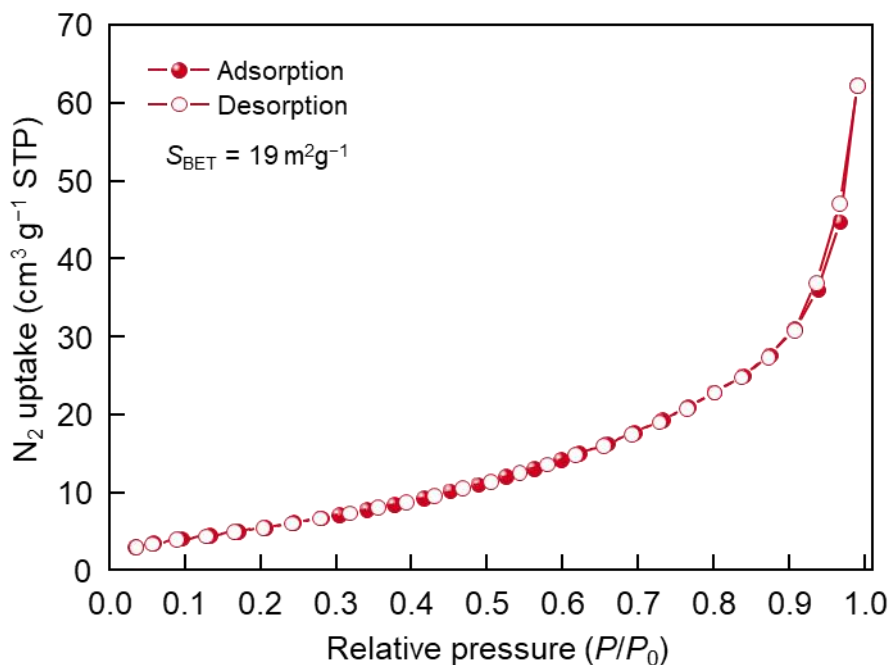


275 **Supplementary Figure 17.** SEM images of acid-digested CPOF-4-265 °C-84 h.

276



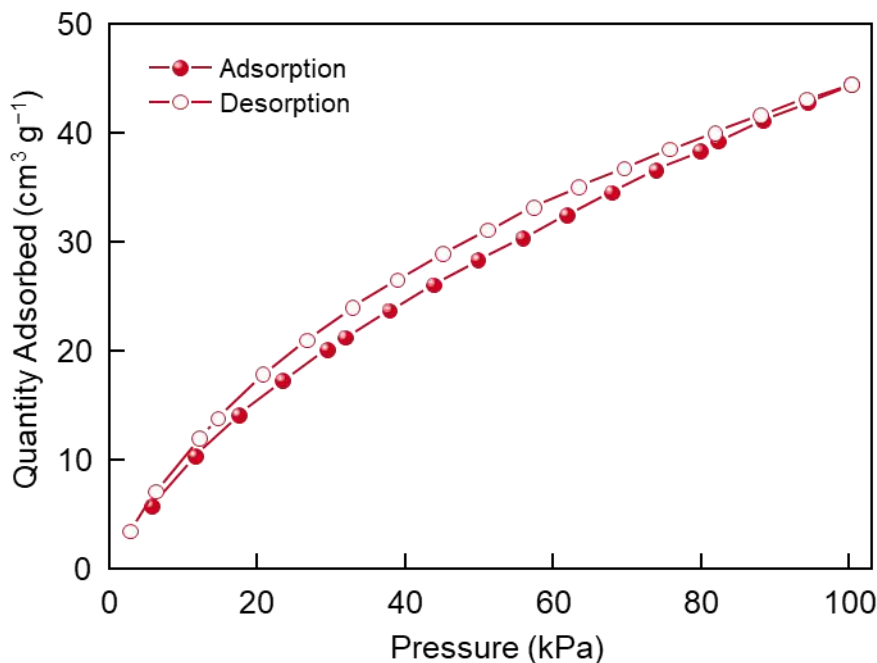
278 **Supplementary Figure 18.** TEM image of acid-digested CPOF-4-265 °C-84 h.



279

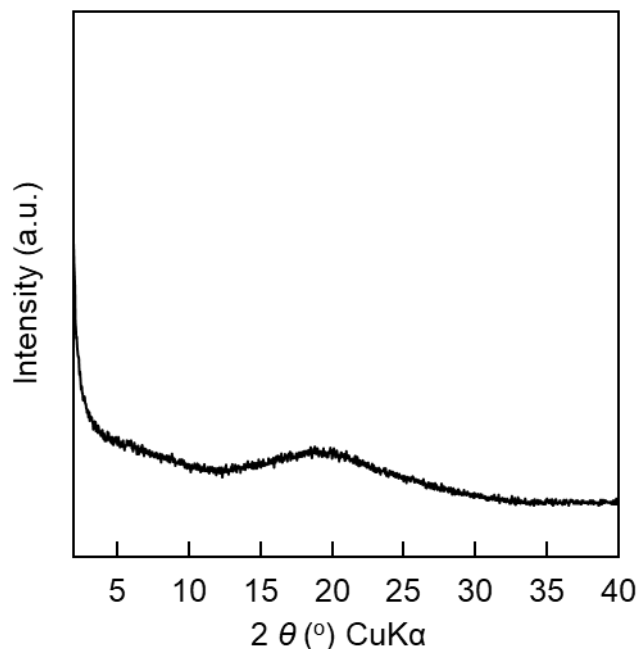
280 **Supplementary Figure 19.** N₂ sorption isotherms of acid-digested CPOF-4-265 °C-84
281 h at 77 K . Solid symbols, adsorption; open symbols, desorption.

282



283

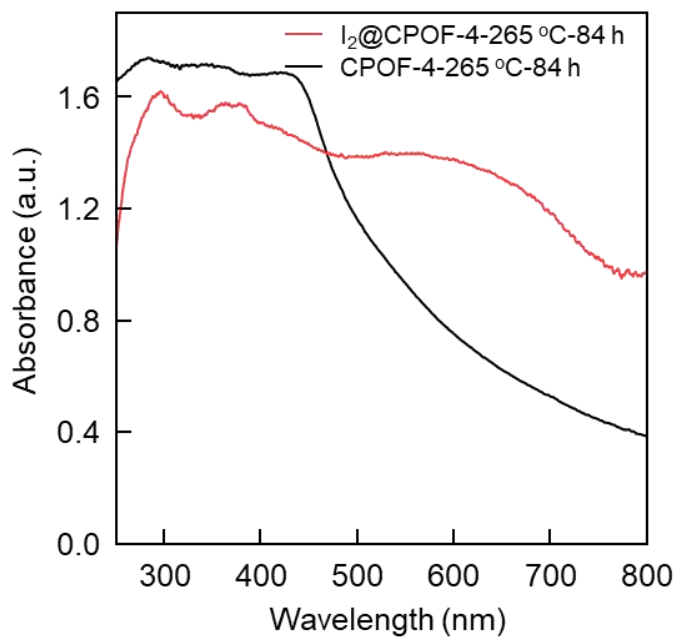
284 **Supplementary Figure 20.** CO₂ sorption isotherms of acid-digested CPOF-4-265
285 °C-84 h at 273 K. Solid symbols, adsorption; open symbols, desorption.



286

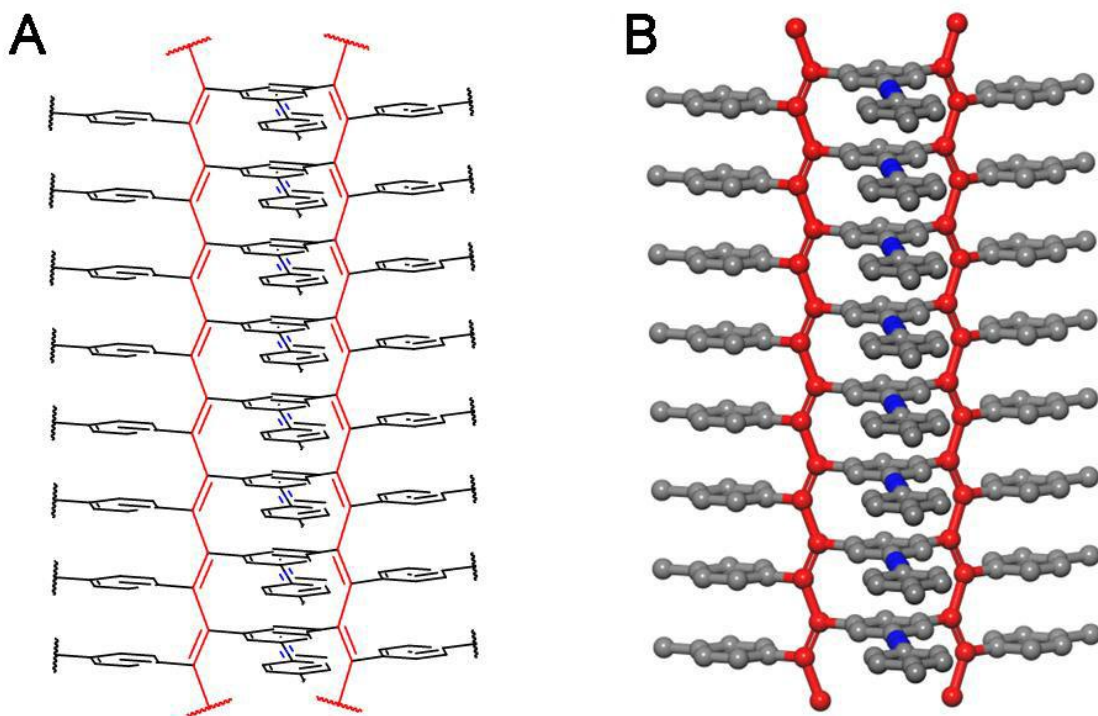
287 **Supplementary Figure 21.** PXRD pattern of acid-digested CPOF-4-265 °C-84 h.

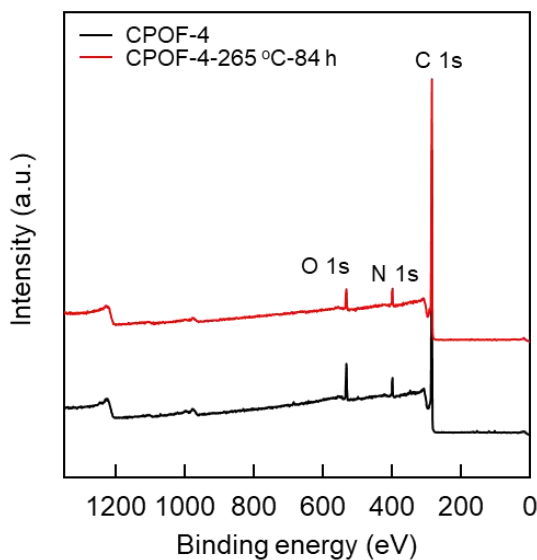
288



289

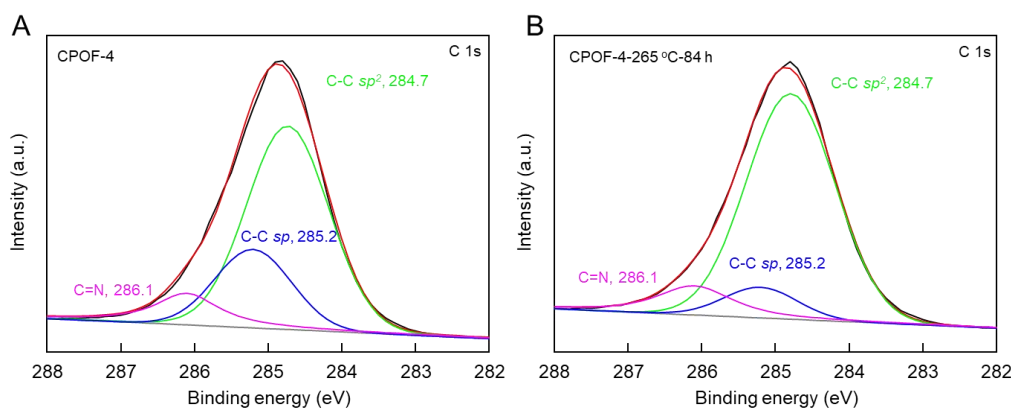
290 **Supplementary Figure 22.** Changes of UV-vis absorption spectra upon gas-phase
291 iodine doping for the CPOF-4-265 °C-84 h. After doping with iodine, the absorption
292 band at 250-420 nm, assigned to a $\pi-\pi^*$ transition in conjugated structure, slightly
293 decreased in intensity. At the same time, due to the polaron electron transition another
294 new absorption appeared at \sim 600 nm.



301 **Section S6. X-ray photoelectron spectroscopy**

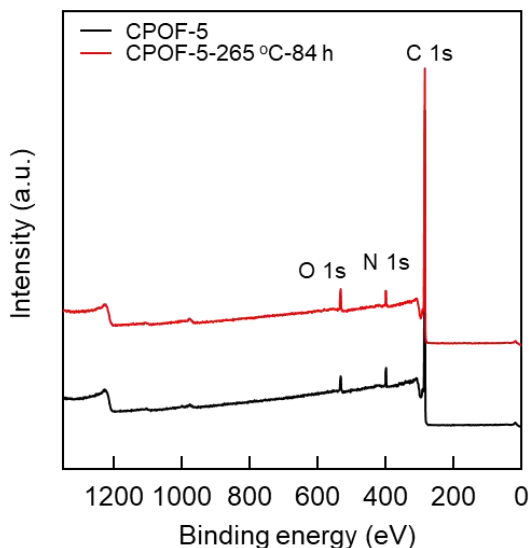
302

303 **Supplementary Figure 24.** XPS spectra of CPOF-4 (black), CPOF-4-265 °C-84 h
304 (red).



305

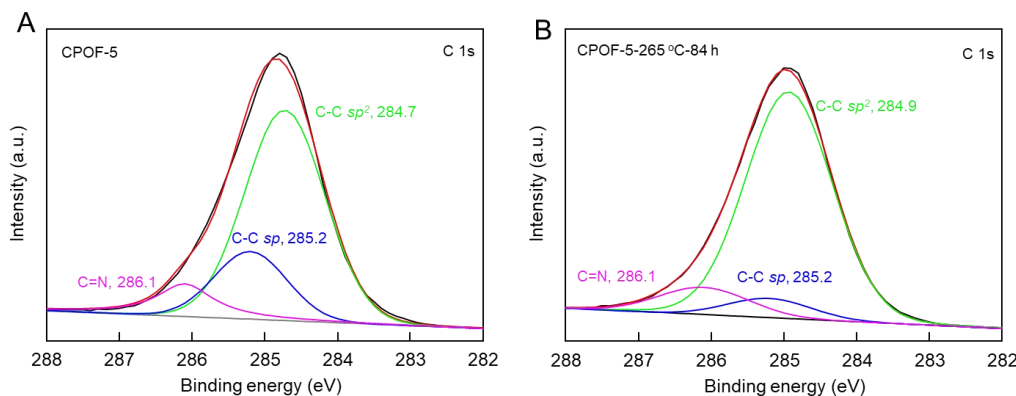
306 **Supplementary Figure 25.** High-resolution C 1s XPS peak of CPOF-4 (A),
307 CPOF-4-265 °C-84 h (B).



308

309 **Supplementary Figure 26.** XPS spectra of CPOF-5 (black), CPOF-5-265 °C-84 h
310 (red).

311



312

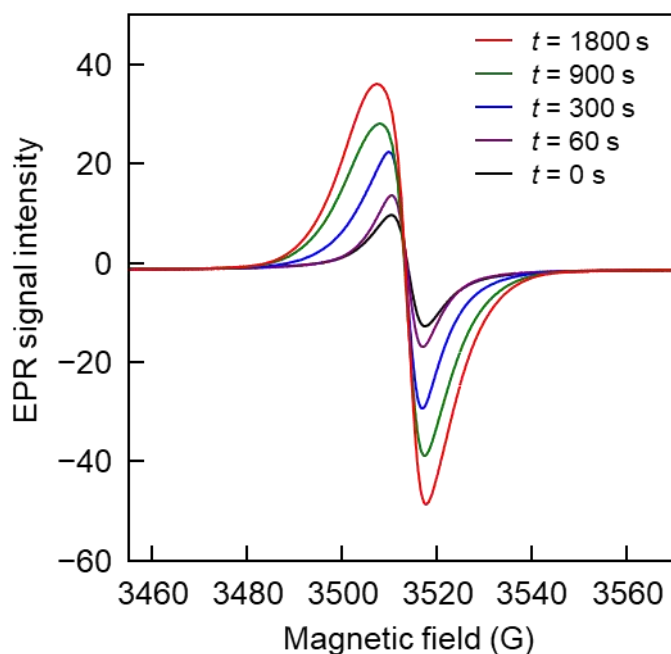
313 **Supplementary Figure 27.** High-resolution C 1s XPS peak of CPOF-5 (A),
314 CPOF-5-265 °C-84 h (B).

315 **Supplementary Table 1.** The atomic percentage of different C species in the sample.

Samples	Name	Peak maximum	Peak area	Atomic %
CPOF-4	C=C <i>sp</i> ²	284.73	148945.2	65.23
	C≡C <i>sp</i>	285.2	52991.19	23.21
	C=N	286.1	26389.14	11.56
CPOF-4-265 °C-84 h	C=C <i>sp</i> ²	284.79	171800.4	79.50
	C≡C <i>sp</i>	285.2	18989.14	8.79
	C=N	286.1	25309.97	11.71
CPOF-5	C=C <i>sp</i> ²	284.73	174267.1	69.15
	C≡C <i>sp</i>	285.2	49809.73	19.77
	C=N	286.1	27926.8	11.08
CPOF-5-265 °C-84 h	C=C <i>sp</i> ²	284.93	195285.2	83.34
	C≡C <i>sp</i>	285.2	15607.03	6.67
	C=N	286.1	23427.21	9.99

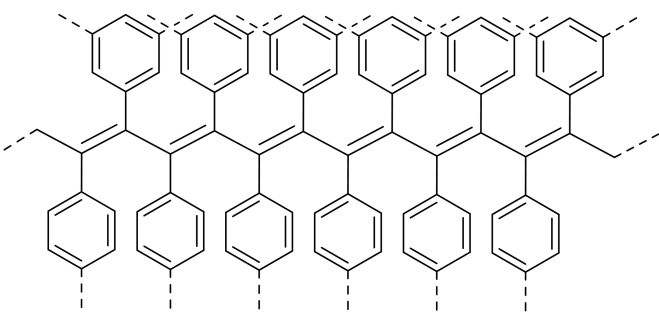
316

317 **Section S7. Electron paramagnetic resonance**



318

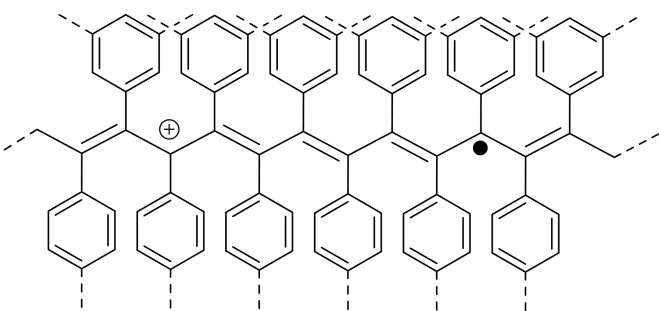
319 **Supplementary Figure 28.** EPR signal for CPOF-4-265 °C-84 h sample as a function
320 of time after I₂ exposure at room temperature.



321

322 **Supplementary Figure 29.** Proposed chemical structure of disubstituted polyacetylene
323 in CPOF-4-265 °C-84 h.

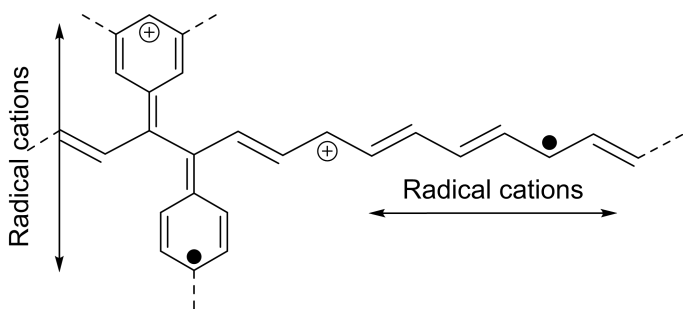
324



325

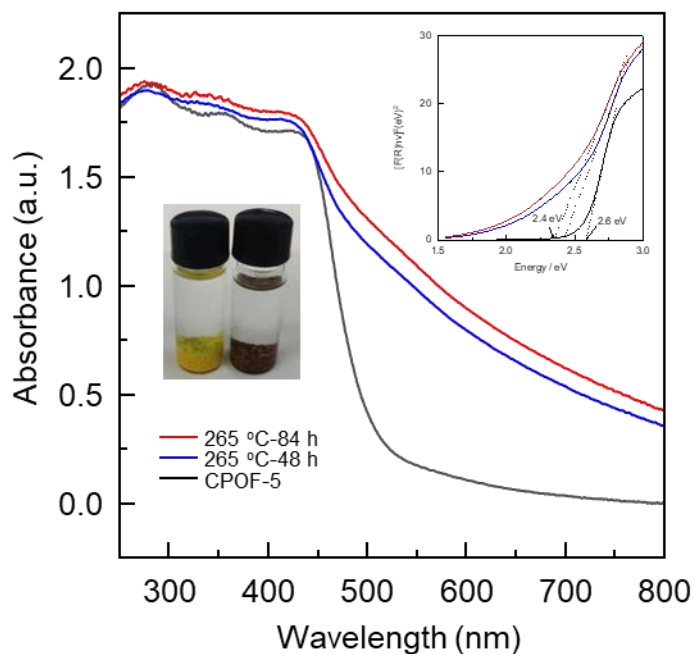
326 **Supplementary Figure 30.** Generation of charge carriers along the main chain after
327 doping with iodine.

328



329

330 **Supplementary Figure 31.** Radical cations in the CPOF-4-265 °C-84 h.

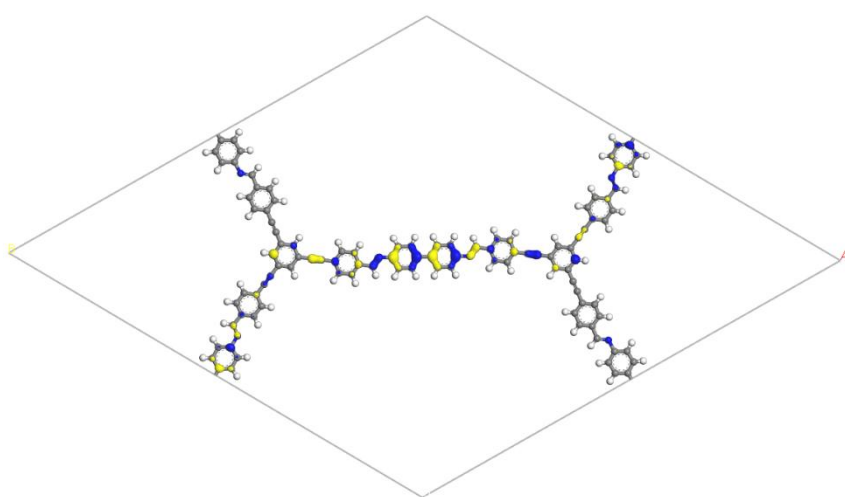
331 **Section S8. UV-visible spectra**

332

333 **Supplementary Figure 32.** UV-vis Diffuse Reflection Spectroscopy (DRS) of CPOF-5,
334 CPOF-5-265 °C-48 h and CPOF-5-265 °C-84 h. Inset: plot of Kubelka–Munk function
335 to determine the band gap of CPOF-5, CPOF-5-265 °C-48 h and CPOF-5-265 °C-84 h.
336

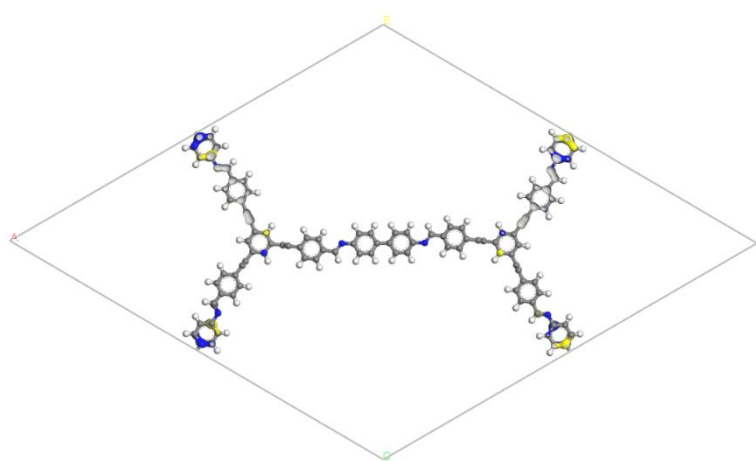
337 Section S9. Density Functional Theory Calculations

338 It is worth noting that even after a long time of reaction, the final conversion rate of
339 CPOF-4 is only about 60~70%. We speculate that about two-thirds of the acetylene
340 groups in CPOF-4 have reacted. Considering these factors, we directly connected
341 acetylenic groups between adjacent layers on the basis of the original CPOF-4 structure,
342 while retaining one-third of the acetylenic groups, and further optimized the structure to
343 obtain the CPOF-4-265 °C-48 h model with a conversion rate of two-thirds. Then, the
344 frontier orbitals of CPOF-4 and CPOF-4-265 °C-48 h were calculated by density
345 functional theory calculations (DFT).



346

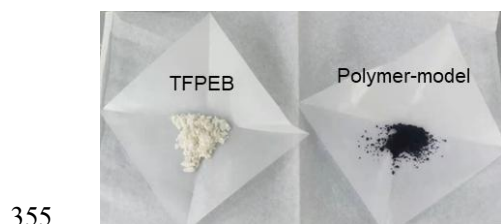
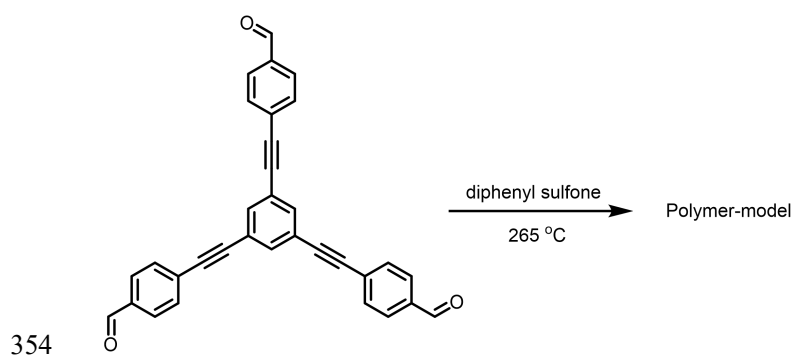
347 **Supplementary Figure 33.** The isosurface of the electron wavefunction of the HOMO
348 of CPOF-4.



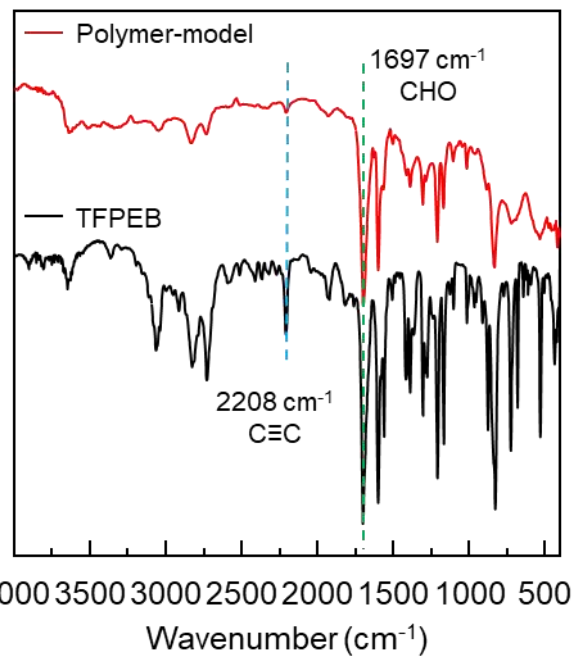
349

350 **Supplementary Figure 34.** The isosurface of the electron wavefunction of the HOMO
351 of CPOF-4-265 °C-48 h.

352

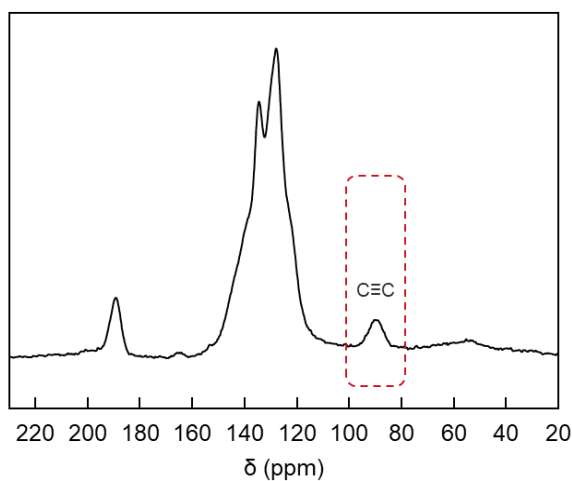
353 **Section S10. Synthesis of polymer-model**

356 A 5 mL vial charged with TFPPEB (100.0 mg) and diphenyl sulfone (3 g), The vial was
357 then transferred to a tubular furnace and evacuated-filled with N₂ by five cycles.
358 subsequently, the temperature was raised to 265 °C at the rate of 10 °C/min in N₂
359 flowing atmosphere with the flow rate of 20 mL/min, and kept at 265 °C for 24 h. The
360 temperature was reduced to room temperature at the rate of 10 °C/min at the end of the
361 holding time. Finally, the obtained product was washed with THF and acetone to
362 remove the residual diphenyl sulfone, dried at 100 °C under vacuum over-night to
363 afford the polymer-model as a black solid.



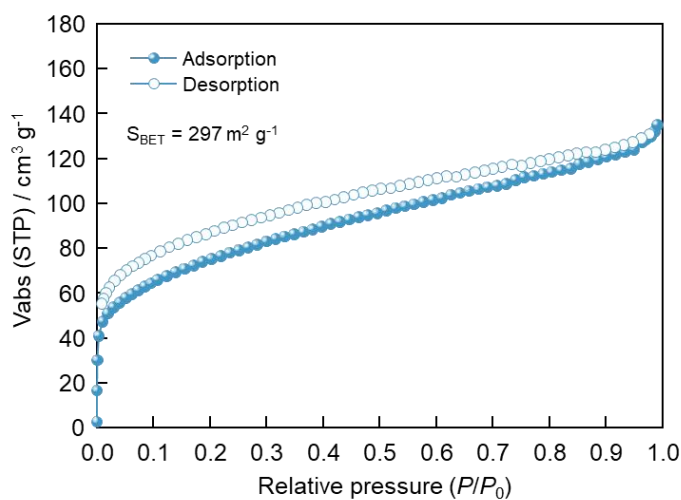
364

365 **Supplementary Figure 35.** FT-IR spectra of 1,3,5-tri(4-formylphenylethyynyl)benzene
366 and polymer-model.



367

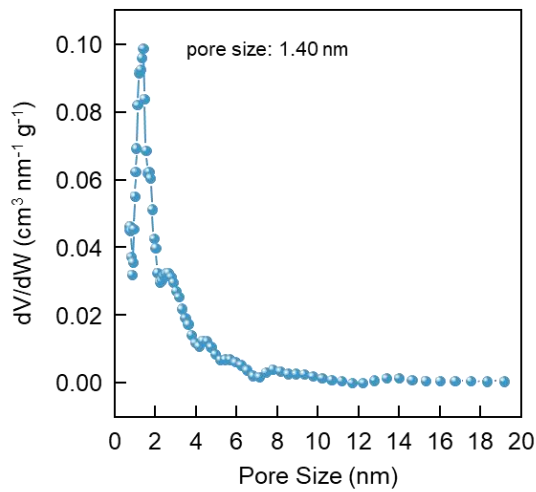
368 **Supplementary Figure 36.** ¹³C CP-MAS NMR spectra of polymer-model.



369

370 **Supplementary Figure 37.** N₂ sorption isotherms of polymer-model: solid symbols,
371 adsorption; open symbols, desorption.

372

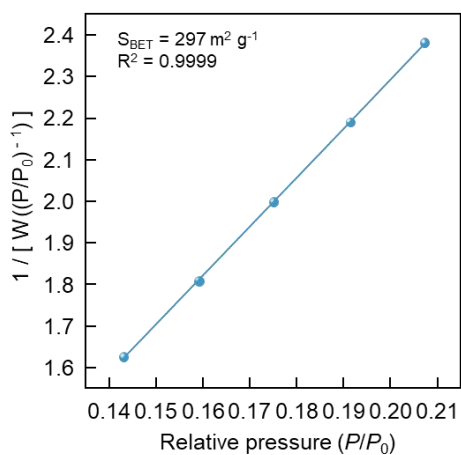


373

374 **Supplementary Figure 38.** The pore size distribution of polymer-model derived from
375 N₂ adsorption calculated by QSDFT method.

376

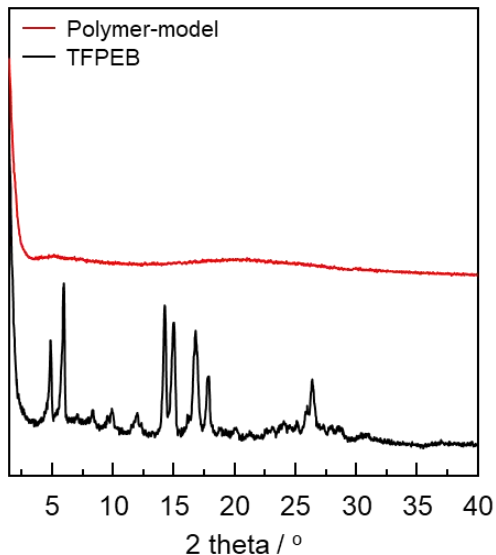
377



378

379 **Supplementary Figure 39.** BET plots of polymer-model calculated from N_2 adsorption
380 isotherm at 77 K.

381



382

383 **Supplementary Figure 40.** PXRD patterns for
384 1,3,5-tri(4-formylphenylethynyl)benzene and polymer-model.

385 **Section S11. PXRD patterns and structures**

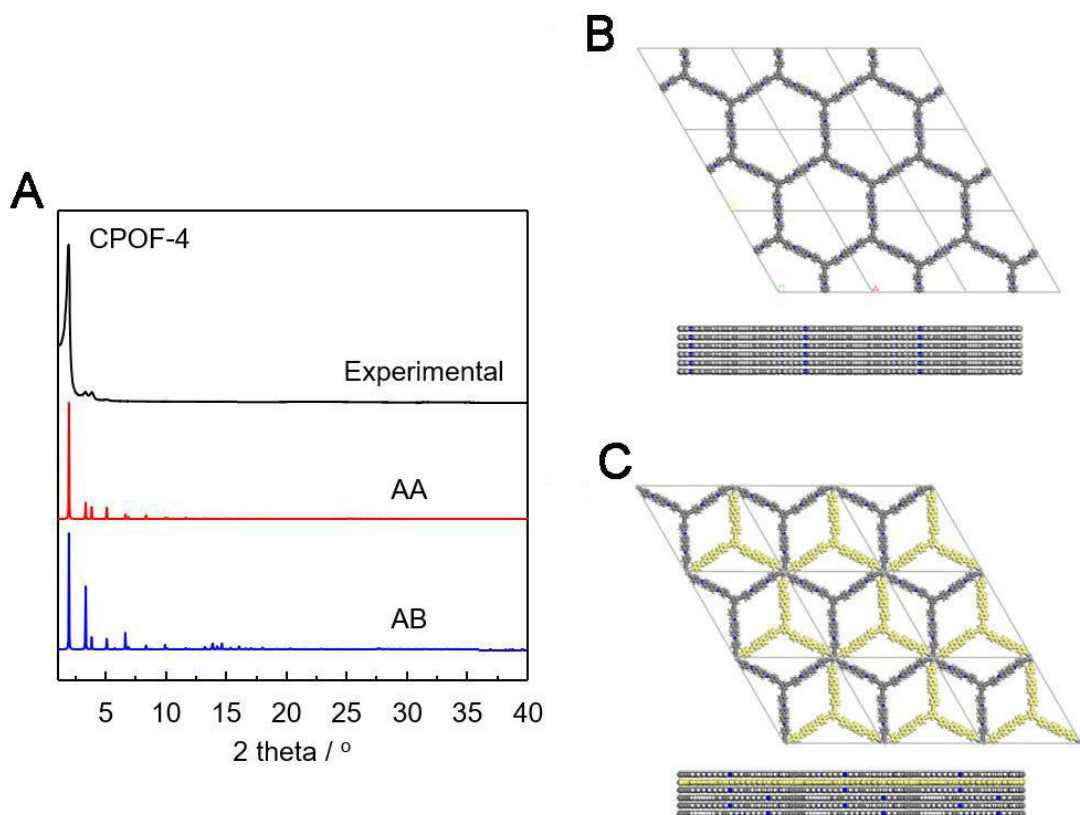
386 Crystal models for 2D COFs and CL-COFs were established by Materials Studio 7.0
387 Software Package. Geometry optimization of the established models was performed by
388 Materials Studio Force Module, which is an advanced classical molecular mechanics
389 tool and allows for fast and reliable geometry optimization and energy calculations.
390 Possible stacking modes were tested. Eclipsed (AA) and slipped (AB) were constructed
391 and optimized in comparison with the experimental Powder X-ray diffraction (PXRD)
392 data. Pawley refinement was carried out using Reflex, a software package for crystal
393 determination from PXRD pattern. The Pawley refinement was performed to optimize
394 the lattice parameters iteratively until the R_{wp} and R_p value converges and the overlay of
395 the observed refined profiles shows good agreement.
396 The structure models of CPOF-4-265 °C-84 h and CPOF-5-265 °C-84 h were
397 determined by directly linking the CPOF-4 and CPOF-5 in the crystallographic
398 *c*-direction and optimizing them in Materials Studio using the Force Module,
399 respectively.
400 We use zero-point energy which calculated by Self-Consistent Field (SCF) to evaluate
401 the stability of the species.

402

403 **Supplementary Table 2.** The Zero Point Energy for CPOF-4 and CPOF-4-265 °C-84 h,
 404 CPOF-5 and CPOF-5-265 °C-84 h, the unit is eV.

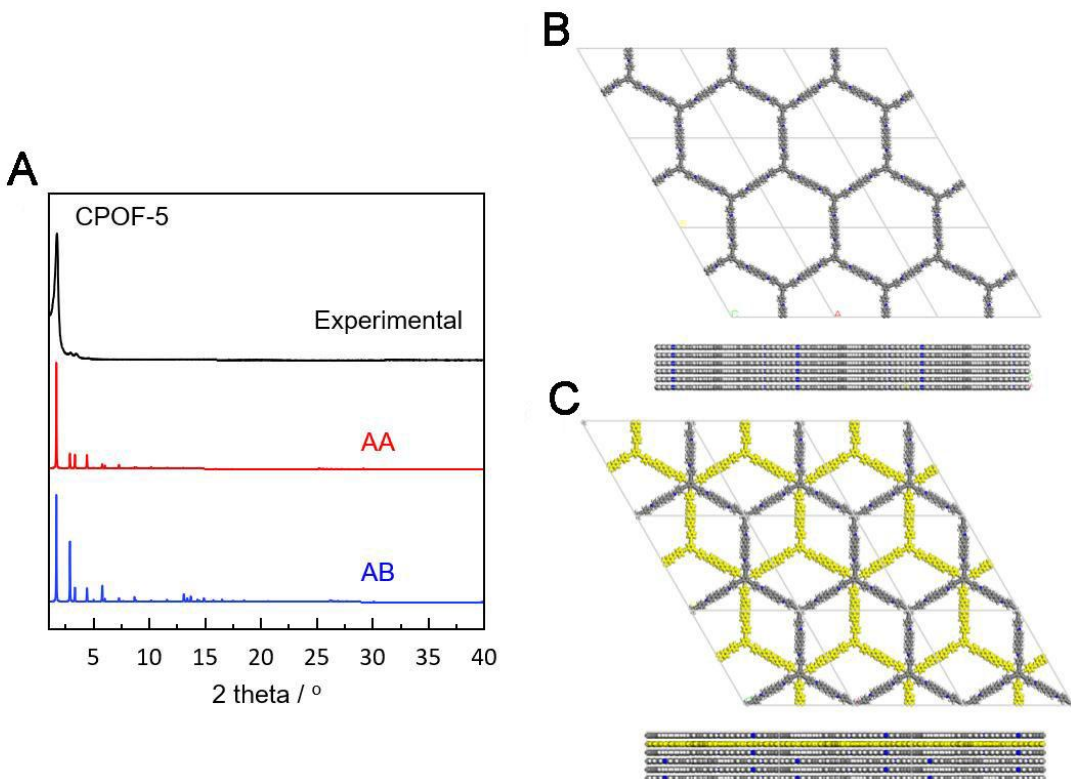
Species	Zero Point Energy (eV)	Difference (eV)
CPOF-4	-2369.8736	
CPOF-4-265 °C-84 h	-2373.1908	-3.3172
CPOF-5	-2785.8982	
CPOF-5-265 °C-84 h	-2790.0196	-4.1214

405 The Density Functional Theory (DFT) which base on first-principles were performed
 406 through the projector augmented wave (PAW) method by using Vienna ab initio
 407 Simulation Package (VASP) code^[2,3]. The results were calculated by self-consistent
 408 field (SCF) method which base on Kohn-Sham equation. The Generalized gradient
 409 approximation (GGA) method with the Perdew-Burke-Ernzerhof (PBE) was adopted as
 410 the exchange-correlation functional. All the calculation uses gamma-centered k-points
 411 $1 \times 1 \times 7$ based on Monkhorst–Pack kpoint grids, DFT-D3 method with Becke-Johnson
 412 damping function, 600 eV cutoff energy and the spin-polarized calculations (collinear).
 413 The convergence tolerance for the residual force and energy on each atom during
 414 structure relaxation were set to 0.05 eV Å⁻¹ and 10⁻⁵ eV.

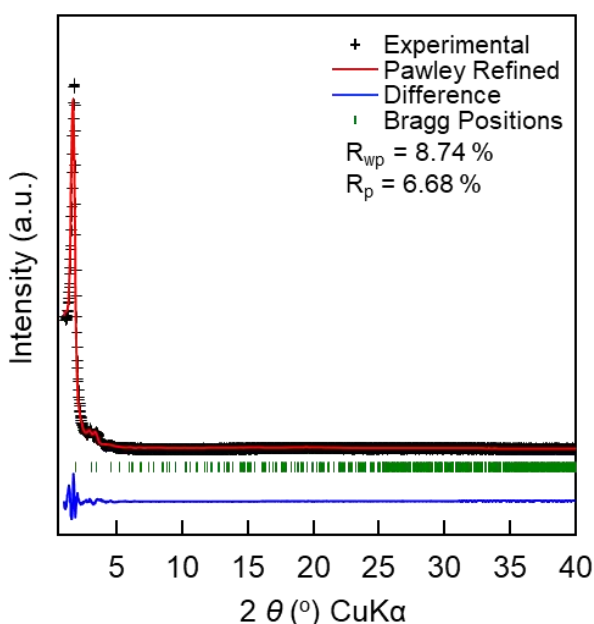


415

416 **Supplementary Figure 41.** (A) XRD profiles of CPOF-4: experimental (black),
417 simulated by using AA-stacking (red) models and AB-stacking (blue) models; (B) Unit
418 cells of AA-stacking modes; (C) Unit cells of AB-stacking modes.

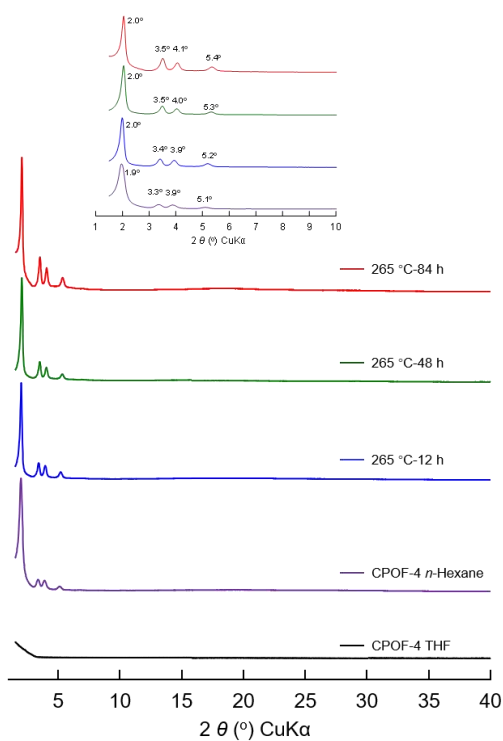


419
420 **Supplementary Figure 42.** (A) XRD profiles of CPOF-5: experimental (black),
421 simulated by using AA-stacking (red) models and AB-stacking (blue) models; (B) Unit
422 cells of AA-stacking modes; (C) Unit cells of AB-stacking modes.
423



424
425 **Supplementary Figure 43.** PXRD profiles of CPOF-5. experimentally observed
426 results (black), Pawley refined (red), their difference (blue) and Bragg positions
427 (green).
428

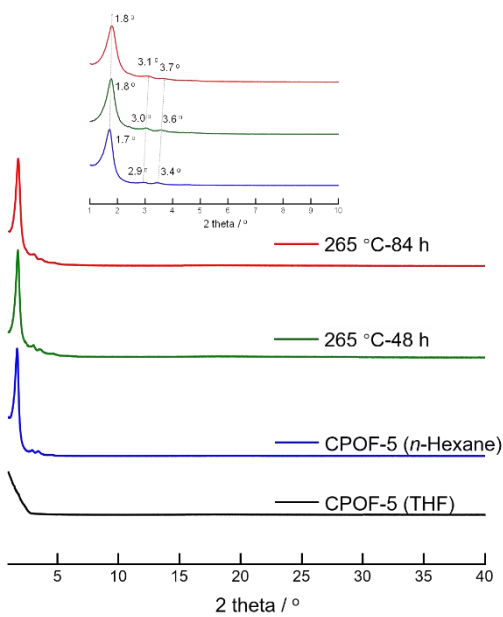
429



430

431 **Supplementary Figure 44.** PXRD spectra of CPOF-4 (THF), CPOF-4 (*n*-hexane),
432 CPOF-4-265 °C-12 h, CPOF-4-265 °C-48 h, and CPOF-4-265 °C-84 h.

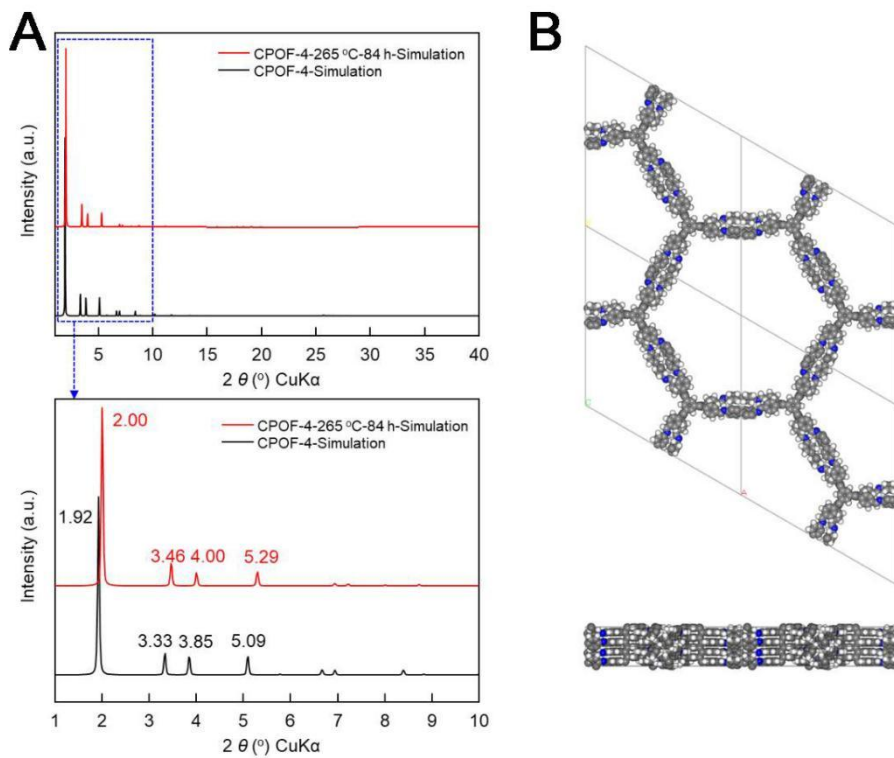
433



434

435 **Supplementary Figure 45.** PXRD spectra of CPOF-5 (THF), CPOF-5 (*n*-hexane),
436 CPOF-5-265 °C-48 h, and CPOF-5-265 °C-84 h.

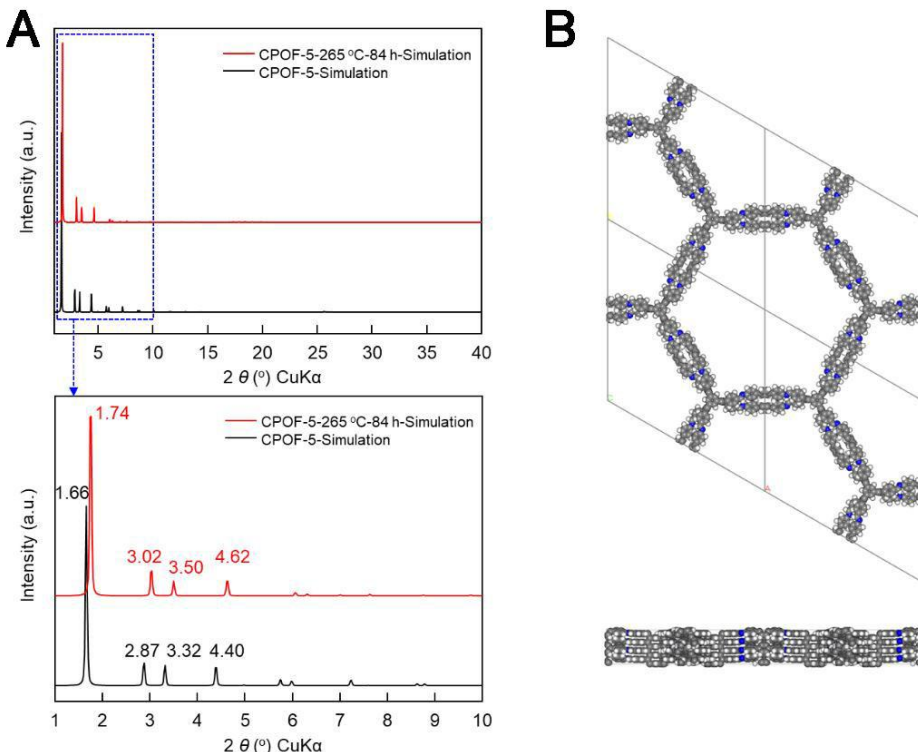
437



438

439 **Supplementary Figure 46.** (A) Simulated PXRD patterns of CPOF-4 (black) and
 440 CPOF-4-265 °C-84 h (red); (B) Schematic representation of CPOF-4-265 °C-84 h.

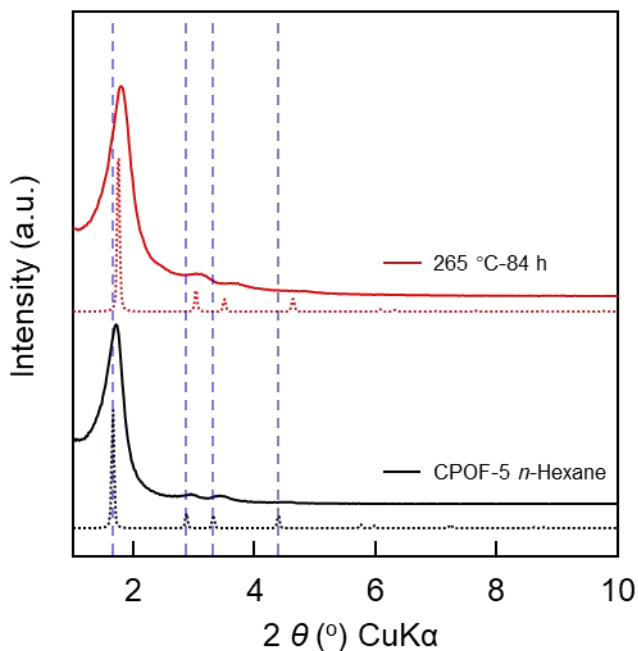
441



442

443 **Supplementary Figure 47.** (A) Simulated PXRD patterns of CPOF-5 (black) and
 444 CPOF-5-265 °C-84 h (red); (B) Schematic representation of CPOF-5-265 °C-84 h.

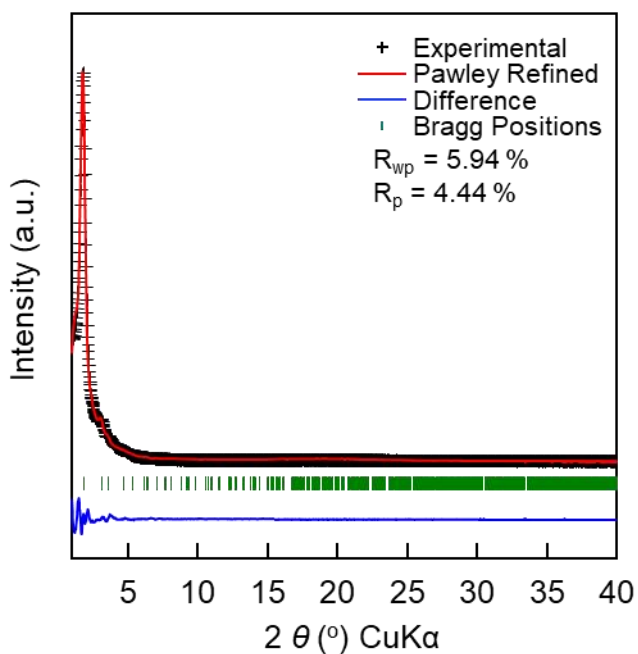
445



446

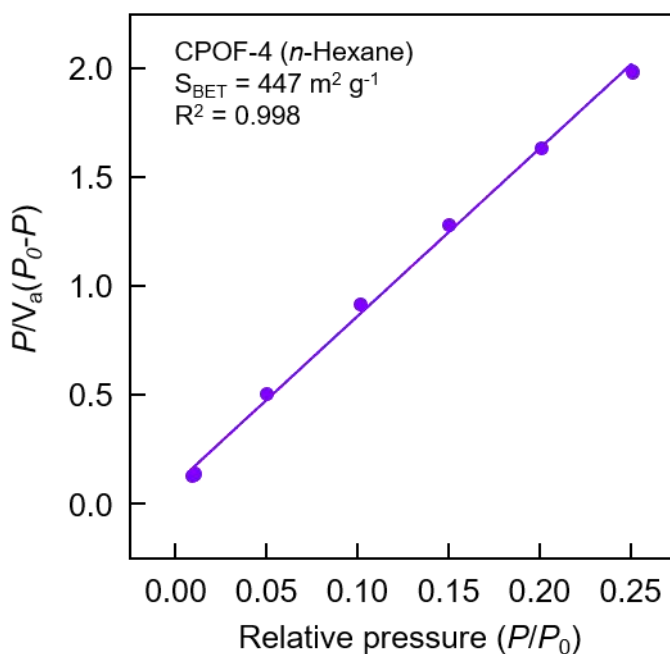
447 **Supplementary Figure 48.** PXRD patterns of CPOF-5 and CPOF-5-265 °C-84 h:
448 experimentally observed (solid line) and simulated based on eclipsed stacking modes
449 (dashed line).

450



451

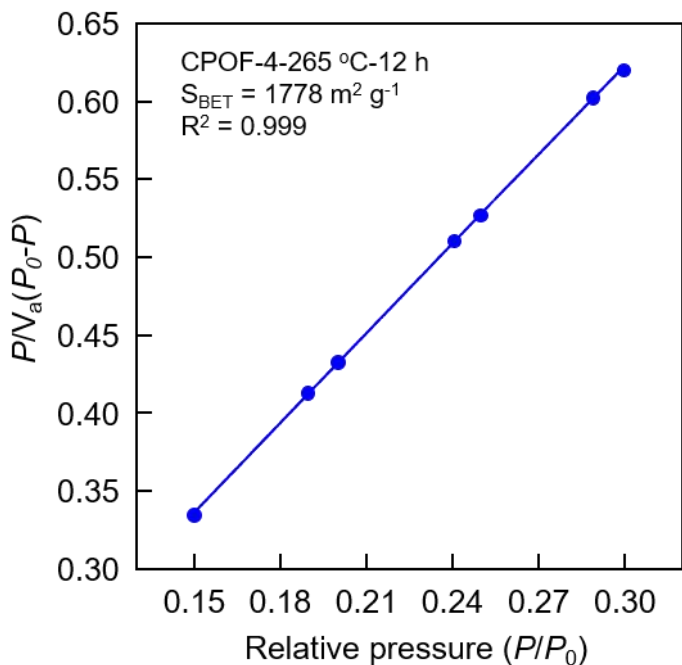
452 **Supplementary Figure 49.** PXRD patterns of CPOF-5-265 °C-84 h: comparison
453 between the experimental (black) and Pawley refined (red) profiles, the refinement
454 differences (blue), and the Bragg positions (green).

455 **Section S12. Nitrogen adsorption**

456

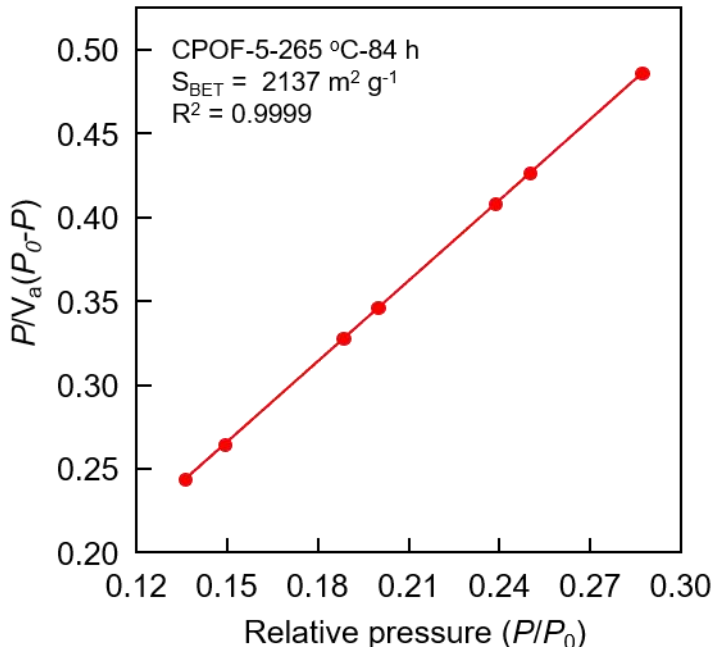
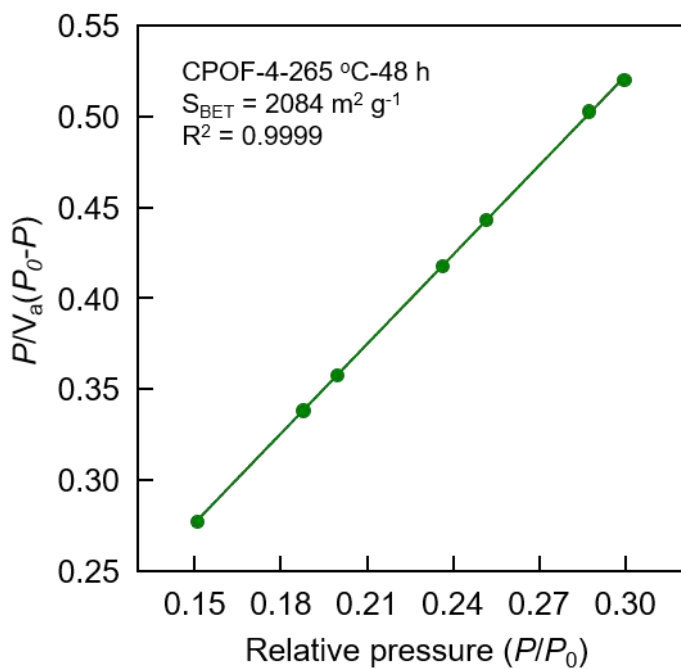
457 **Supplementary Figure 50.** BET plots of CPOF-4 (n-hexane) calculated from N₂
458 adsorption isotherm at 77 K.

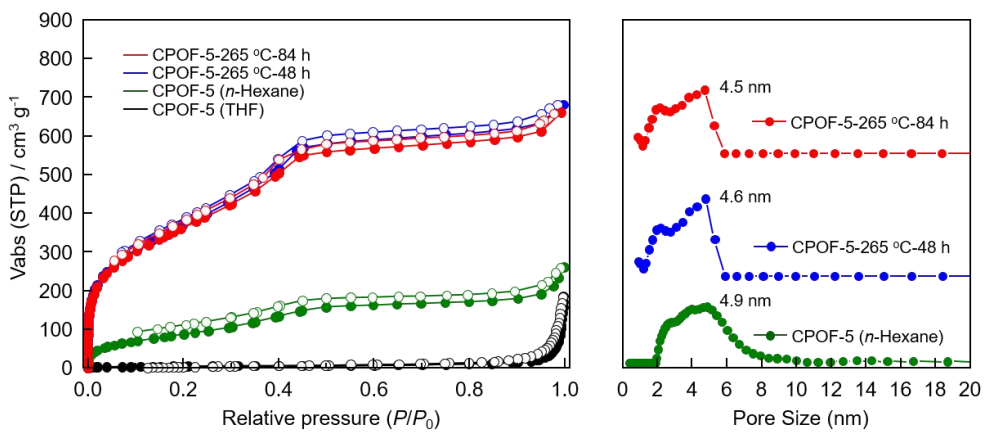
459



460

461 **Supplementary Figure 51.** BET plots of CPOF-4-265 °C-12 h calculated from N₂
462 adsorption isotherm at 77 K.



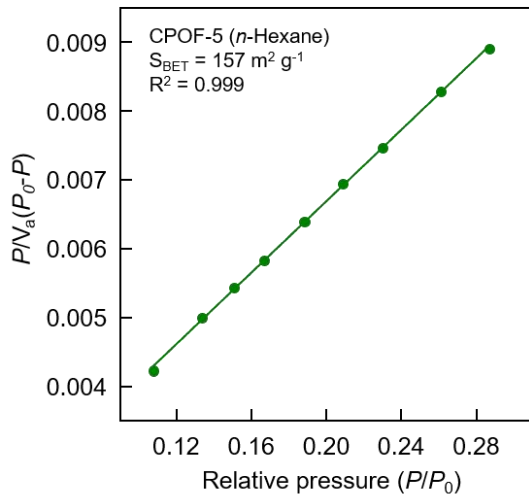


470

471 **Supplementary Figure 54.** N₂ sorption isotherms of CPOF-5 (THF), CPOF-5
 472 (n-hexane), CPOF-5-265 °C-48 h, and CPOF-5-265 °C-84 h: solid symbols, adsorption;
 473 open symbols, desorption. The pore size distribution derived from N₂ adsorption
 474 calculated by QS-DFT method.

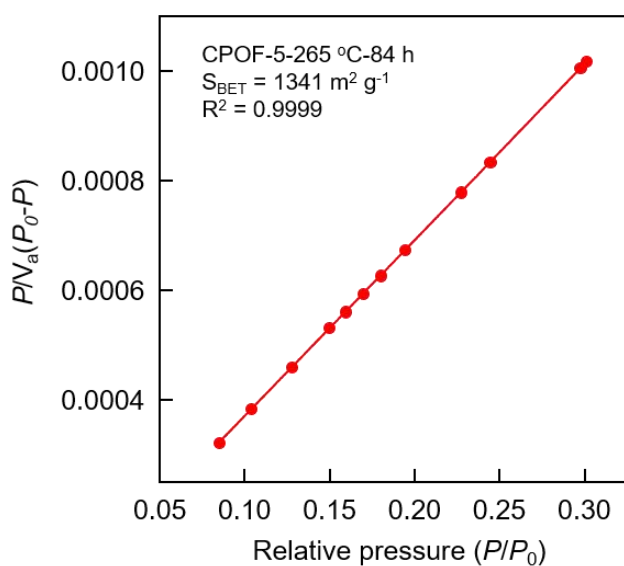
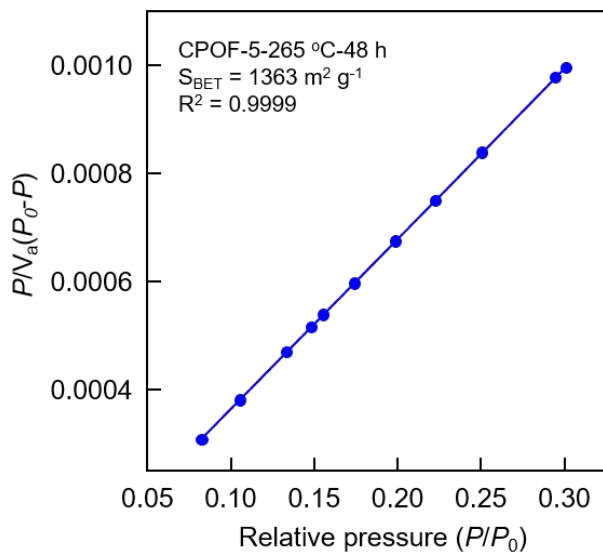
475

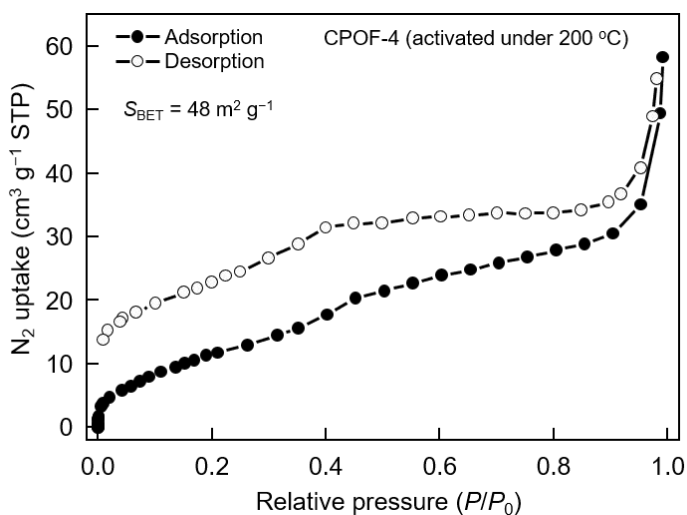
476



477

478 **Supplementary Figure 55.** BET plots of CPOF-5 (n-hexane) calculated from N₂
 479 adsorption isotherm at 77 K.

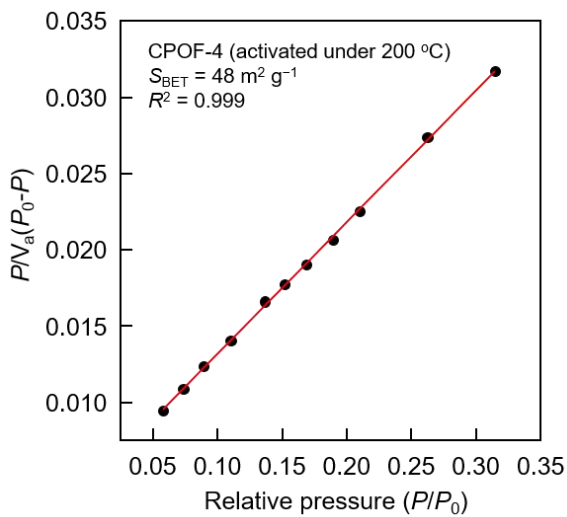




487

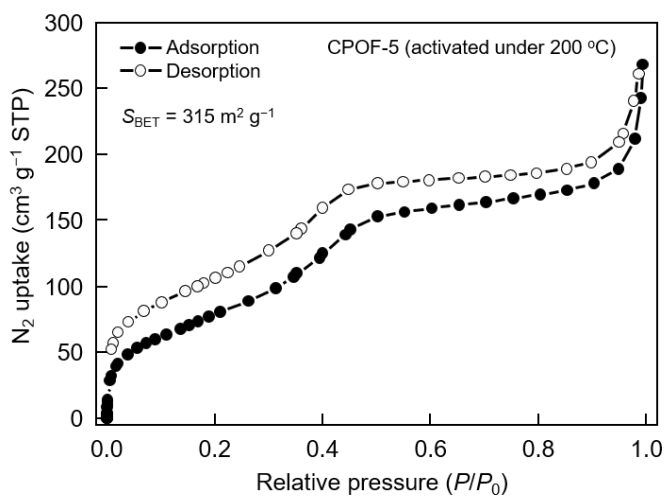
488 **Supplementary Figure 58.** N_2 sorption isotherms of CPOF-4 (activated under 200 °C):
489 solid symbols, adsorption; open symbols, desorption.

490



491

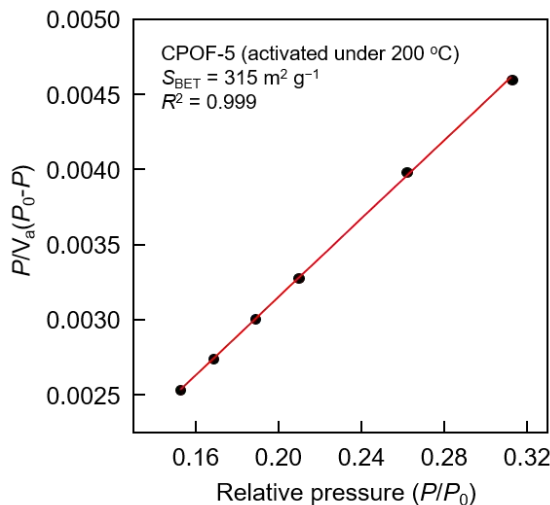
492 **Supplementary Figure 59.** BET plots of CPOF-4 (activated under 200 °C) calculated
493 from N_2 adsorption isotherm at 77 K.



494

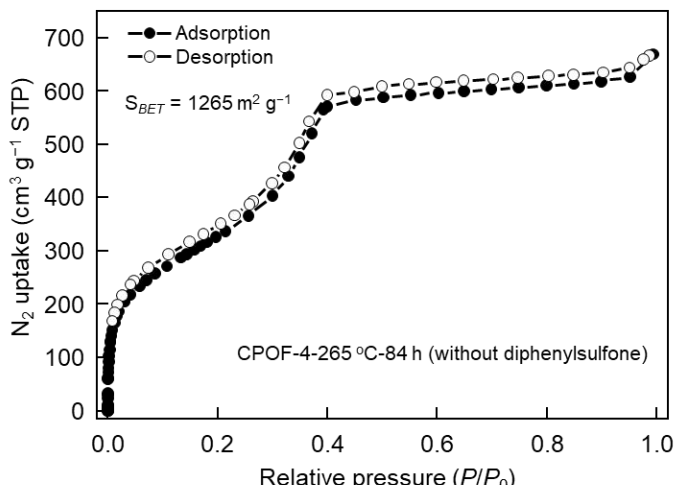
495 **Supplementary Figure 60.** N₂ sorption isotherms of CPOF-5 (activated under 200 °C):
496 solid symbols, adsorption; open symbols, desorption.

497



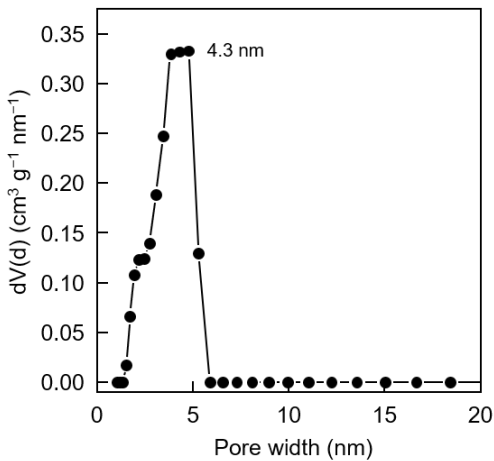
498

499 **Supplementary Figure 61.** BET plots of CPOF-5 (activated under 200 °C) calculated
500 from N₂ adsorption isotherm at 77 K.



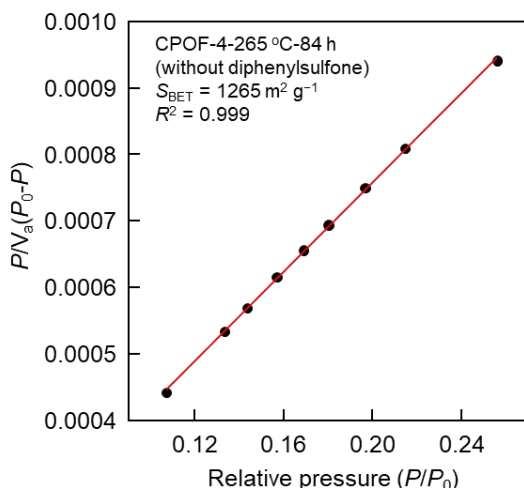
501

Supplementary Figure 62. N_2 sorption isotherms of CPOF-4-265 °C-84 h (without phenyl sulfone): solid symbols, adsorption; open symbols, desorption.



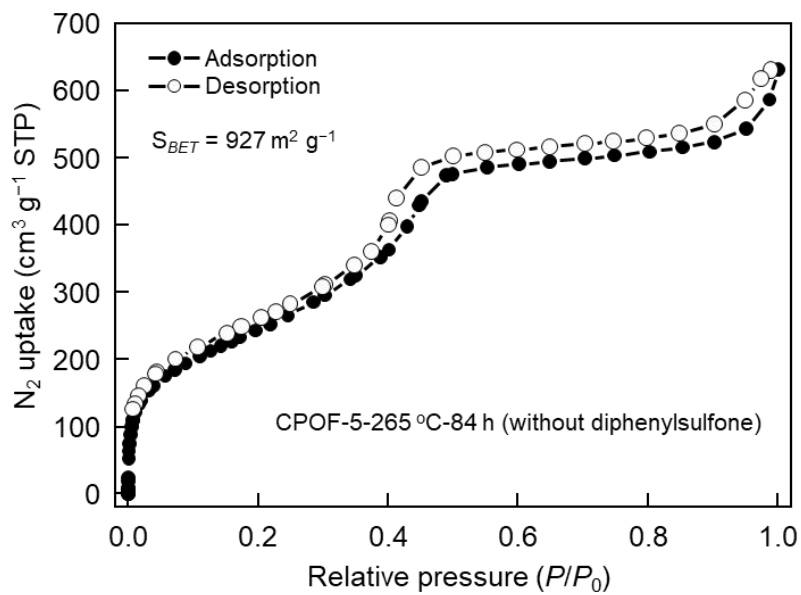
504

Supplementary Figure 63. The pore size distribution of CPOF-4-265 °C-84 h (without phenyl sulfone): derived from N_2 adsorption calculated by QSDFT method.



507

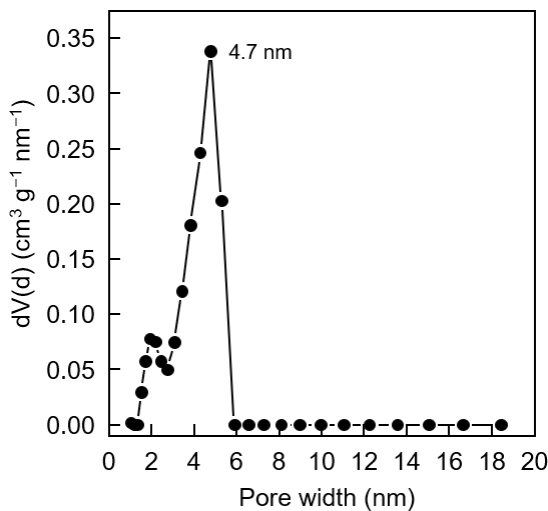
Supplementary Figure 64. BET plots of CPOF-4-265 °C-84 h (without phenyl sulfone): calculated from N_2 adsorption isotherm at 77 K.



510

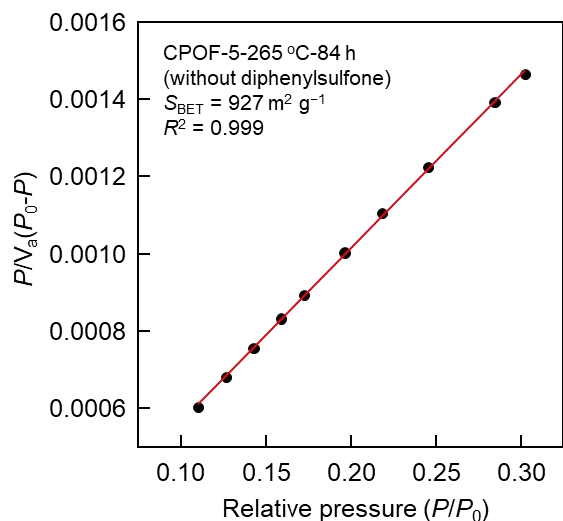
511 **Supplementary Figure 65.** N_2 sorption isotherms of CPOF-5-265 °C-84 h (without
512 phenyl sulfone): solid symbols, adsorption; open symbols, desorption.

513



514

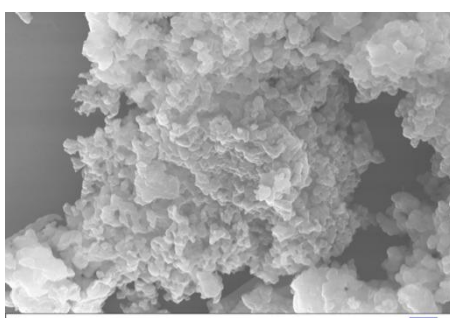
515 **Supplementary Figure 66.** The pore size distribution of CPOF-5-265 °C-84 h (without
516 phenyl sulfone): derived from N_2 adsorption calculated by QS-DFT method.



517

518 **Supplementary Figure 67.** BET plots of CPOF-5-265 °C-84 h (without phenyl
519 sulfone): calculated from N₂ adsorption isotherm at 77 K.

520 **Section S13. SEM image**

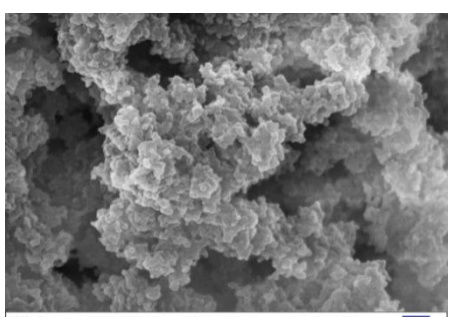


521

1 μm EHT = 10.00 kV Signal A = InLens Date: 9 May 2022
WD = 7.3 mm Mag = 10.00 KX Time: 11:37:10 ZEISS

522

Supplementary Figure 68. SEM image of as-synthesized CPOF-4.

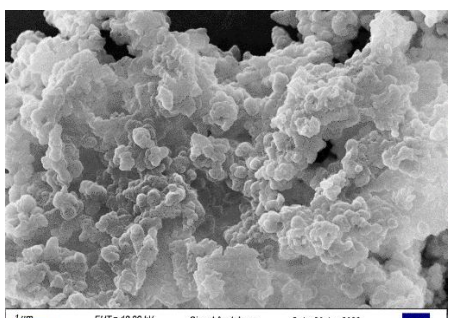


523

300 nm EHT = 10.00 kV Signal A = InLens Date: 2 May 2022
WD = 5.7 mm Mag = 31.00 KX Time: 13:05:27 ZEISS

524

Supplementary Figure 69. SEM image of as-synthesized CPOF-5.

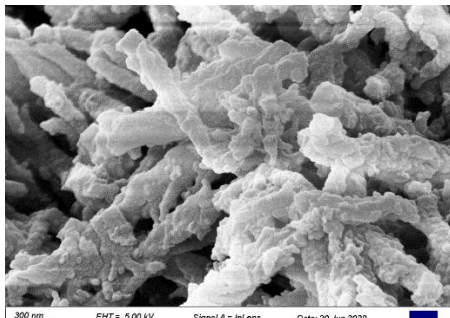


525

1 μm EHT = 10.00 kV Signal A = InLens Date: 20 Jun 2022
WD = 5.8 mm Mag = 11.00 KX Time: 13:01:58 ZEISS

526

Supplementary Figure 70. SEM image of CPOF-4-265 °C-84 h.



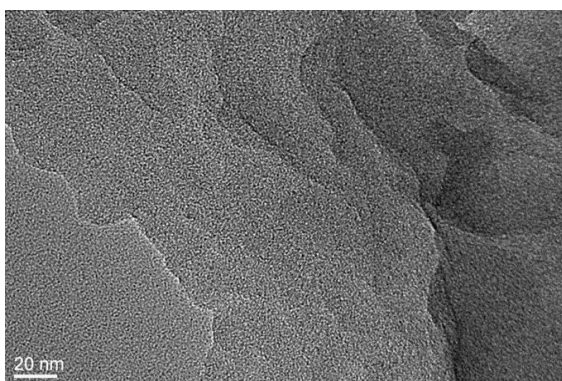
527

300 nm EHT = 5.00 kV Signal A = InLens Date: 20 Jun 2022
WD = 5.8 mm Mag = 31.72 KX Time: 12:50:18 ZEISS

528

Supplementary Figure 71. SEM image of CPOF-5-265 °C-84 h.

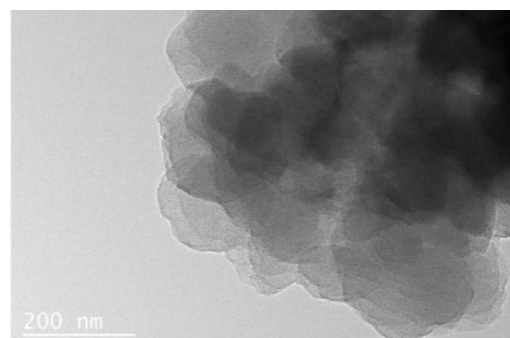
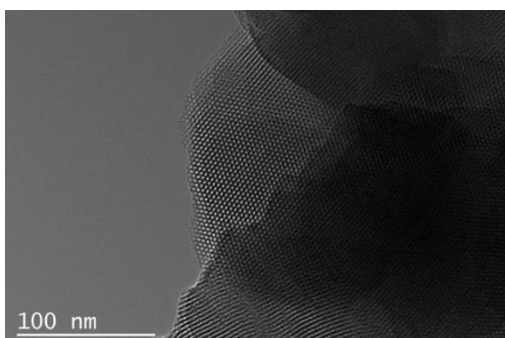
529 **Section S14. TEM image**



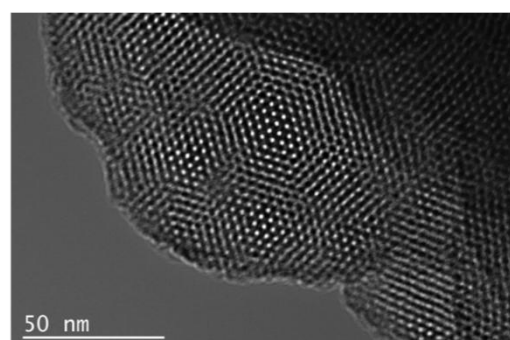
530

531 **Supplementary Figure 72.** TEM image of as-synthesized CPOF-4.

532

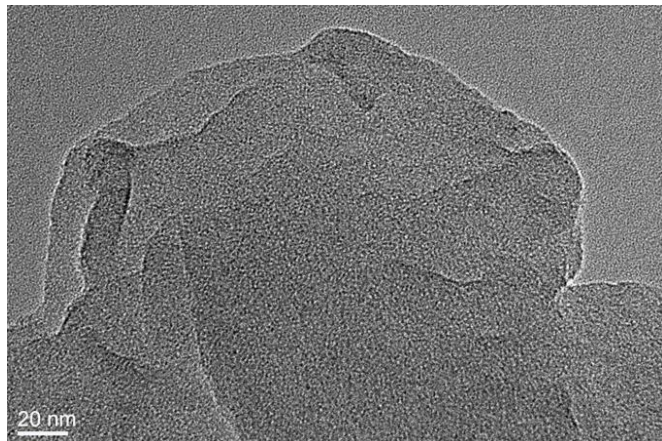


533



534

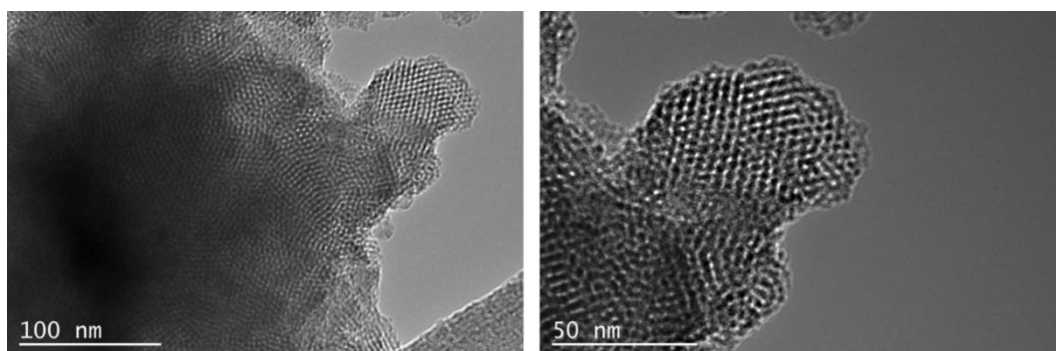
Supplementary Figure 73. TEM image of CPOF-4-265 °C-84 h.



535

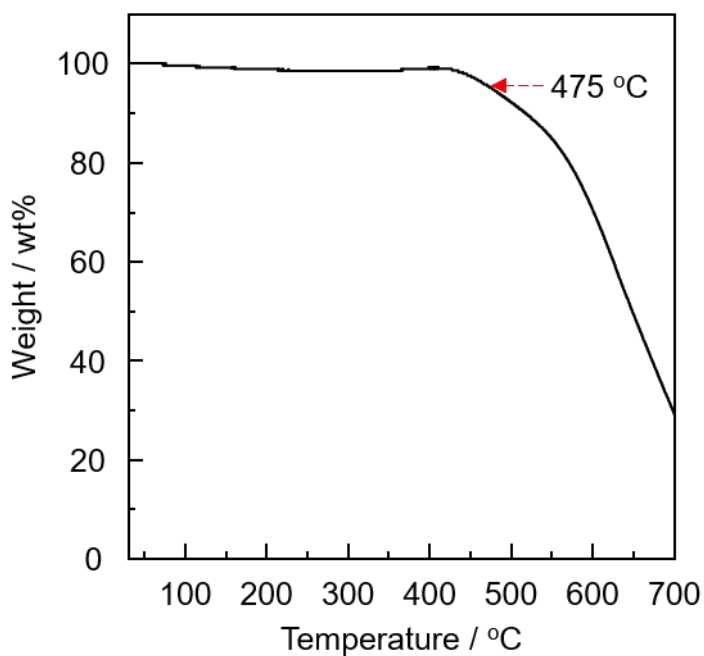
536 **Supplementary Figure 74.** TEM image of as-synthesized CPOF-5.

537



538

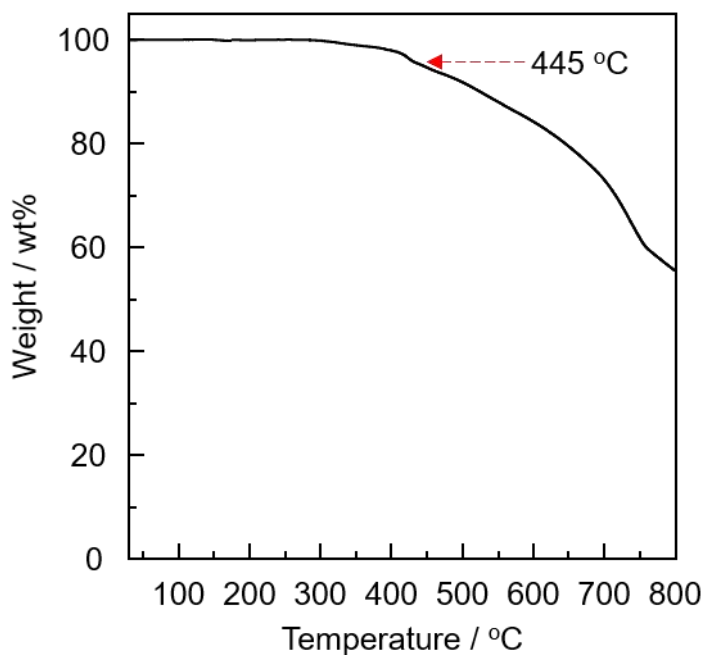
539 **Supplementary Figure 75.** TEM image of CPOF-5-265 °C-84 h.

540 **Section S15. TGA curves**

541

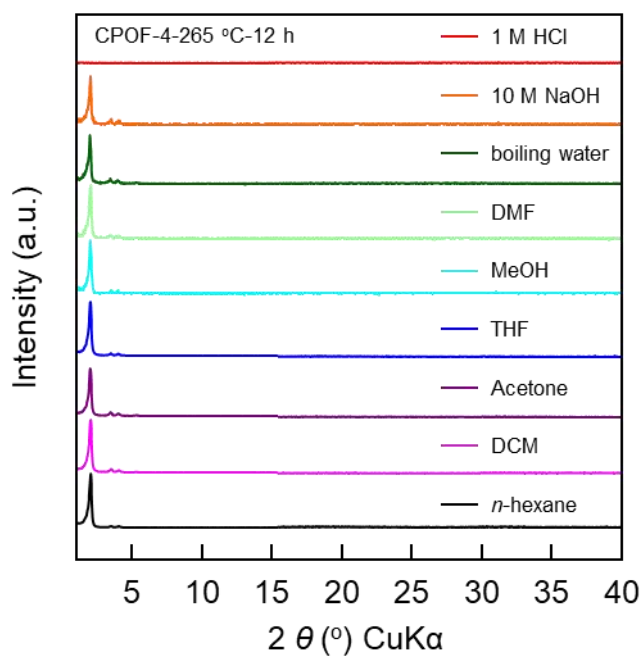
542 **Supplementary Figure 76.** TGA plot of CPOF-4 in N₂ atmosphere, weight loss 5 wt%
543 at 475 °C.

544



545

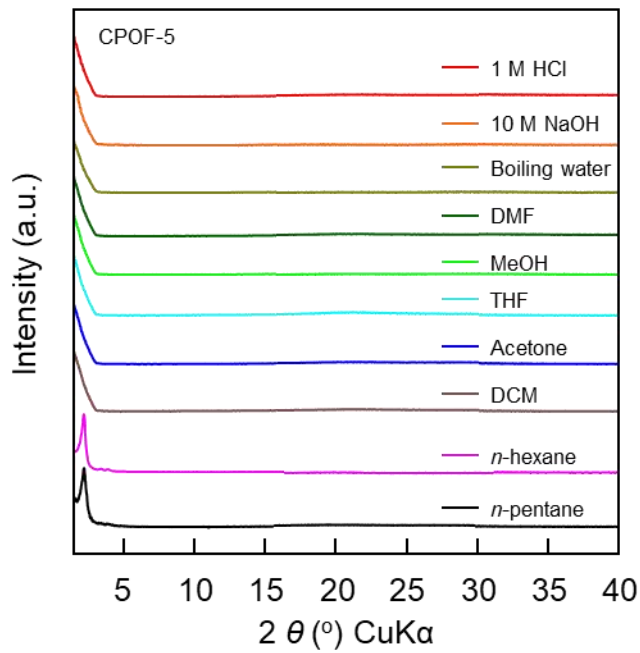
546 **Supplementary Figure 77.** TGA plot of CPOF-5 in N₂ atmosphere, weight loss 5 wt%
547 at 445 °C.

548 **Section S16. Chemical stability tests**

549

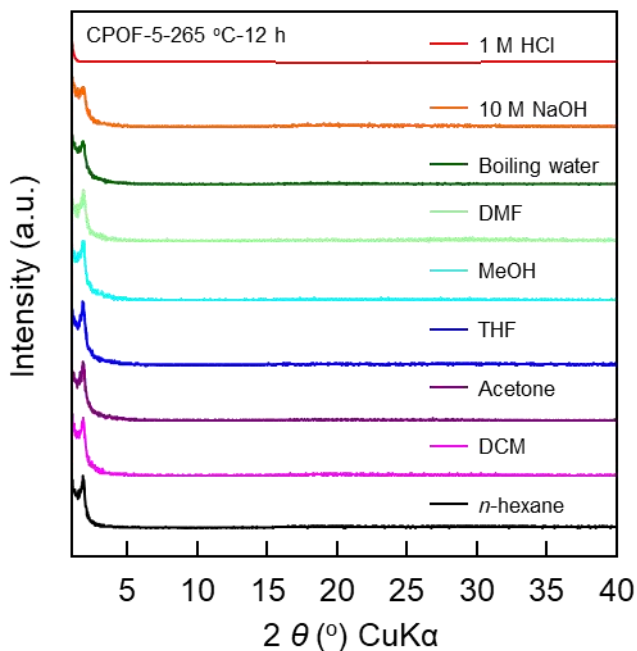
550 **Supplementary Figure 78.** PXRD patterns of CPOF-4-265 °C-12 h after treatments
551 under different chemical environments for 24 h.

552



553

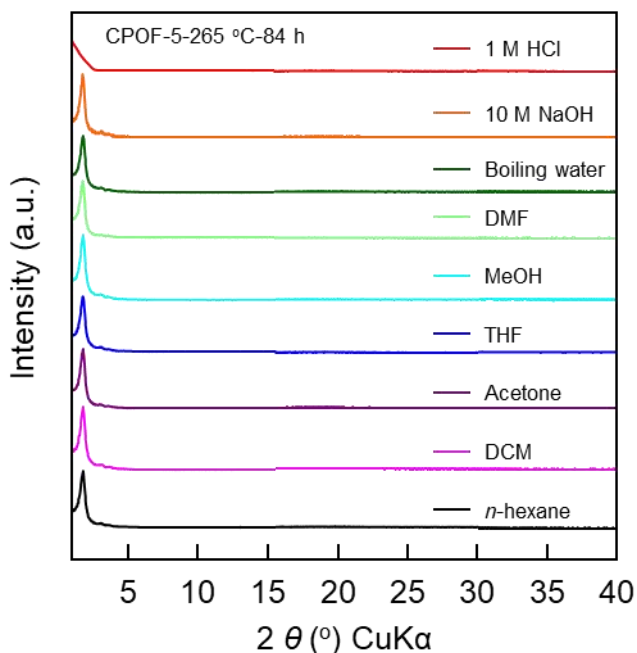
554 **Supplementary Figure 79.** PXRD patterns of CPOF-5 after treatments under different
555 chemical environments for 24 h.



556

557 **Supplementary Figure 80.** PXRD patterns of CPOF-5-265 °C-12 h after treatments
558 under different chemical environments for 24 h.

559



560

561 **Supplementary Figure 81.** PXRD patterns of CPOF-5-265 °C-84 h after treatments
562 under different chemical environments for 24 h.

563 **Section S17. Reaction kinetics and thermodynamic studies**

564 In the in-situ FT-IR spectrum, the absorption peak area is calculated by integrating,
 565 then the reduction of the absorption peak area is proportional to the disappearance of
 566 the corresponding tracking group, and the conversion rate α of the group can be
 567 obtained by the following formula:

568
$$\alpha = \frac{A_0 - A_t}{A_0} \times 100\% \quad (\text{Eq. S1})$$

569 where A_0 is the absorption peak area of the acetylenic groups at the initial time, and A_t
 570 is the absorption peak area of the acetylenic groups at the time t .

571 Quantitative analysis of infrared spectroscopy is based on the Lambert-Beer law, and
 572 the absorbance A is proportional to the measured component concentration c and the
 573 optical path length b of the incident light passing through the sample, that is:

574
$$A = abc \quad (\text{Eq. S2})$$

575 where a is the molar absorption coefficient. At constant optical path length, the
 576 measured A is only related to the type a and concentration c of the component. Thus,
 577 Eq. S2 can be transformed re-written as follow:

578

579
$$A = Kc \quad (K = ab, \text{ is a constant}) \quad (\text{Eq. S3})$$

580 From the rate equation of the chemical reaction, the consumption rate of acetylenic
 581 groups in 2D COFs can be expressed by:

582

583
$$r = -\frac{dc}{dt} = kc^n \quad (\text{Eq. S4})$$

584 where n is the reaction order; k is the reaction rate constant. Thus, Eq. S4 can be
 585 transformed re-written as Eq. S5.

586
$$r = -\frac{1}{K} \frac{dA}{dt} = k \frac{1}{K^n} A^n - \frac{dA}{dt} = k K^{1-n} A^n \quad (\text{Eq. S5})$$

587 where A is the characteristic peak absorbance of acetylenic groups. When the reaction
 588 rate is independent of the concentration of the substance, the reaction follows a
 589 zero-order reaction model. Thus, Eq. S5 can be transformed re-written as follow:

590

591
$$r = kK \quad (\text{Eq. S6})$$

592 The integral of the above equation can be transformed into:

593
$$A = kKt \quad (\text{Eq. S7})$$

594

595 Since the absorbance of the acetylene group is directly proportional to its concentration
596 Thus, Eq. S7 can be transformed re-written as Eq. S8.

597

598 $c = kt$ (Eq. S8)

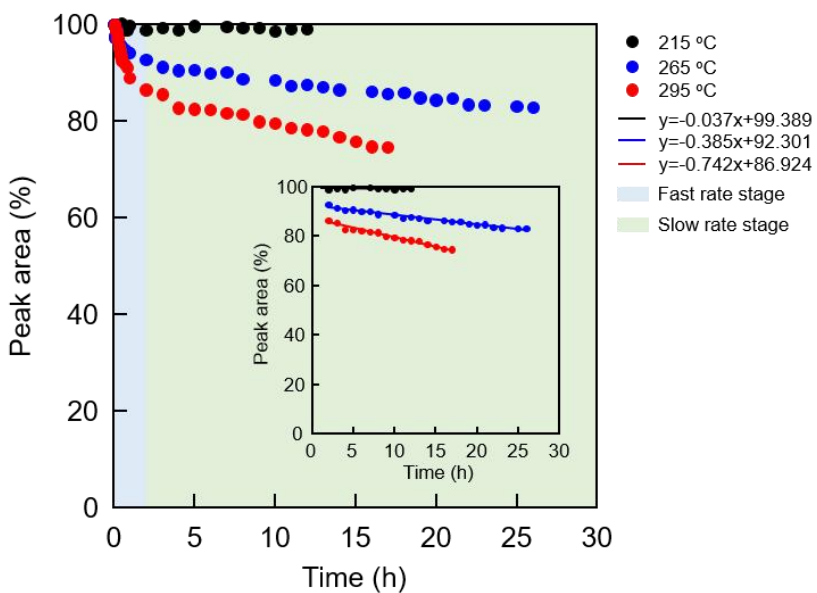
599 The rate constant k values at each reaction temperature obtained from the slope of each
600 straight line are listed in Supplementary Table 3.

601

602 **Supplementary Table 3.** Constants of rate at various temperatures

Temperature (°C)	$k (A \text{ h}^{-1})$
215	0.037
265	0.385
295	0.742

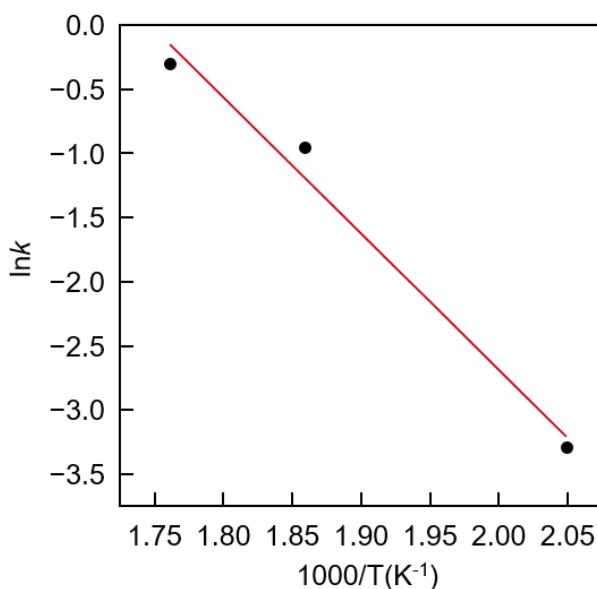
603



604

605 **Supplementary Figure 82.** In-situ variable temperature FT-IR of CPOF-4 at 215 °C,
 606 265 °C and 295 °C respectively.

607

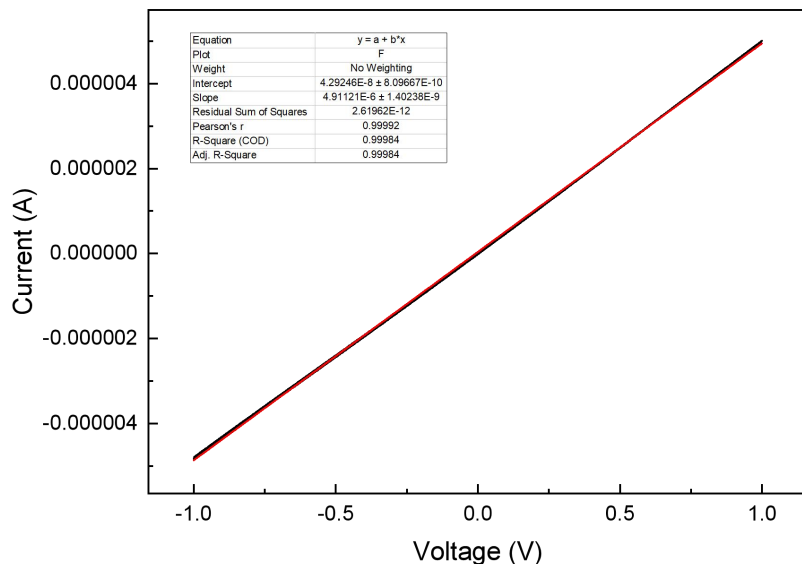


608

609 **Supplementary Figure 83.** Relationship between constants of rate and temperature.

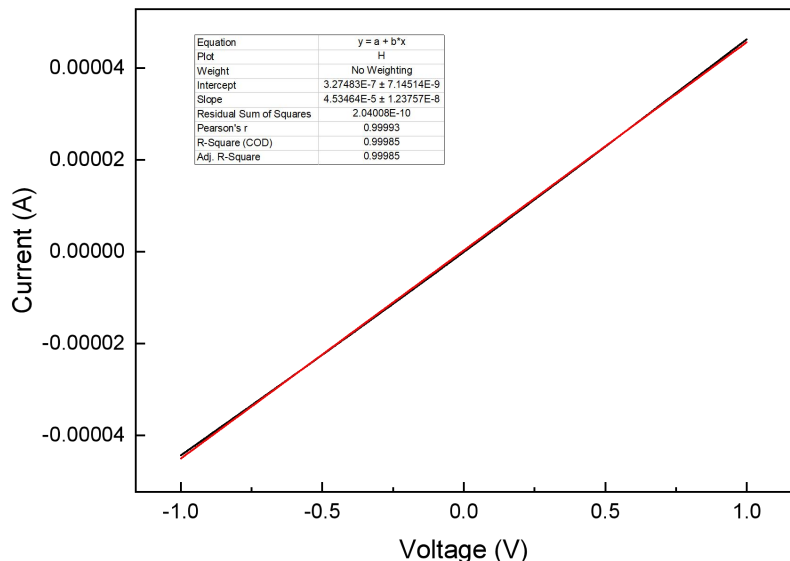
610 **Section S18. Electrical conductivity measurements**

611 **Iodine doping:** A 20 mL brown vial was charged with 5 g iodine. A small vial (5 mL)
 612 charged with the powder of CPOF-4 or CPOF-4-265 °C-84 h was left into the brown
 613 vial, which was further capped tightly and kept in the dark at 75 °C for 24 h. After the
 614 doping samples were cooled to room temperature, a certain number of doping samples
 615 were separated for further experiments^[4-7].



616

617 **Supplementary Figure 84.** I-V curves of I₂@CPOF-4.



618

619 **Supplementary Figure 85.** I-V curves of I₂@CPOF-4-265 °C-84 h.

620 **Section S19. Unit cell parameters and fractional atomic coordinates**

621 **Supplementary Table 4.** Unit cell parameters and fractional atomic coordinates for
 622 CPOF-4 calculated based on the slipped AA stacking mode.

Space group		<i>P</i> 6/ <i>m</i>	
Unit cell		$a = b = 53.8678 \text{ \AA}$, $c = 3.4685 \text{ \AA}$, $\alpha = \beta = 90^\circ$, $\gamma = 120^\circ$	
Pawley refinement		$R_p = 3.12\%$, $R_{wp} = 4.74\%$	
Atoms	x	y	z
C	0.32133	0.68449	0.00000
C	0.35116	0.69650	0.00000
C	0.27288	0.64235	0.00000
C	0.24722	0.63202	0.00000
H	0.31204	0.69830	0.00000
C	0.58990	0.39114	0.00000
C	0.57790	0.40891	0.00000
C	0.59565	0.43891	0.00000
C	0.62552	0.45072	0.00000
C	0.63748	0.43291	0.00000
C	0.61970	0.40310	0.00000
C	0.58352	0.45815	0.00000
N	0.55594	0.44776	0.00000
C	0.54092	0.46357	0.00000
C	0.55482	0.49363	0.00000
C	0.53898	0.50772	0.00000
C	0.50861	0.49236	0.00000
C	0.49511	0.46207	0.00000
C	0.51105	0.44810	0.00000
H	0.57596	0.36809	0.00000
H	0.55479	0.39917	0.00000
H	0.63961	0.47374	0.00000
H	0.66058	0.44238	0.00000
H	0.59821	0.48099	0.00000

H	0.57789	0.50664	0.00000
H	0.55129	0.53075	0.00000
H	0.47220	0.44839	0.00000
H	0.49996	0.42489	0.00000

623

624 **Supplementary Table 5.** Unit cell parameters and fractional atomic coordinates for
 625 CPOF-5 calculated based on the slipped AA stacking mode.

Space group		<i>P</i> 6/ <i>m</i>	
Unit cell		$a = b = 61.4909 \text{ \AA}$, $c = 3.4829 \text{ \AA}$, $\alpha = \beta = 90^\circ$, $\gamma = 120^\circ$	
Pawley refinement		$R_p = 6.68\%$, $R_{wp} = 8.74\%$	
Atoms	x	y	z
C	0.35432	0.63474	0.00000
C	0.34369	0.65092	0.00000
C	0.36323	0.62119	0.00000
C	0.39995	0.61534	0.00000
C	0.41031	0.59962	0.00000
C	0.39464	0.57337	0.00000
C	0.36848	0.56317	0.00000
C	0.35816	0.57892	0.00000
C	0.37387	0.60501	0.00000
N	0.42935	0.56546	0.00000
C	0.40518	0.55643	0.00000
C	0.46856	0.56502	0.00000
C	0.48253	0.55275	0.00000
C	0.47065	0.52620	0.00000
C	0.44404	0.51280	0.00000
C	0.43020	0.52522	0.00000
C	0.44243	0.55154	0.00000
C	0.47393	0.48631	0.00000
C	0.51221	0.52606	0.00000
C	0.48571	0.51276	0.00000
C	0.35943	0.67702	0.00000
H	0.41222	0.63552	0.00000
H	0.43052	0.60786	0.00000
H	0.35606	0.54302	0.00000
H	0.33795	0.57081	0.00000

H	0.39224	0.53646	0.00000
H	0.47815	0.58533	0.00000
H	0.50259	0.56468	0.00000
H	0.43324	0.49263	0.00000
H	0.41001	0.51394	0.00000
H	0.45386	0.47443	0.00000
H	0.52298	0.54623	0.00000
H	0.37963	0.68503	0.00000

626

627 **Supplementary Table 6.** Unit cell parameters and fractional atomic coordinates for
 628 CPOF-4-265 °C-84 h.

Space group		<i>P</i> 1	
Unit cell		$a = 50.9905 \text{ \AA}$, $b = 50.9040 \text{ \AA}$, $c = 5.2398 \text{ \AA}$, $\alpha = 90.0^\circ$, $\beta = 90.4^\circ$, $\gamma = 119.9^\circ$	
Pawley refinement		$R_p = 3.65\%$, $R_{wp} = 5.47\%$	
Atoms	x	y	z
C	0.31433	0.68140	0.48147
C	0.34622	0.69679	0.48263
C	0.26406	0.63379	0.48422
C	0.24924	0.63171	0.25208
C	0.57449	0.36052	0.15211
C	0.55133	0.36821	0.14680
C	0.55880	0.39881	0.14137
C	0.58926	0.42112	0.14673
C	0.61232	0.41372	0.15094
C	0.60529	0.38337	0.15206
C	0.53676	0.40961	0.11671
C	0.48845	0.40622	0.15006
C	0.49202	0.42636	0.95212
C	0.47567	0.44171	0.95082
C	0.45519	0.43732	0.14721
C	0.45021	0.41566	0.33659
C	0.46662	0.40016	0.33653
C	0.31295	0.63281	0.48113
C	0.29756	0.64936	0.48054
C	0.36053	0.63010	0.48803
C	0.36327	0.61788	0.25629
C	0.64383	0.21293	0.21486
C	0.63536	0.18184	0.21196
C	0.60458	0.15937	0.20715

C	0.58289	0.16841	0.21147
C	0.59107	0.19911	0.21382
C	0.62159	0.22177	0.21431
C	0.59294	0.12637	0.18129
C	0.59506	0.08064	0.20403
C	0.57494	0.06508	0.00197
C	0.55880	0.03341	0.99473
C	0.56233	0.01633	0.18931
C	0.58391	0.03197	0.38327
C	0.60023	0.06387	0.38906
C	0.36141	0.67995	0.48346
C	0.34490	0.64802	0.48220
C	0.36417	0.73037	0.48878
C	0.37651	0.74527	0.25781
C	0.78953	0.43198	0.22461
C	0.81985	0.45614	0.23057
C	0.84392	0.45006	0.23996
C	0.83719	0.41995	0.23796
C	0.80723	0.39608	0.23190
C	0.78303	0.40159	0.22751
C	0.87634	0.47343	0.26229
C	0.91949	0.52301	0.21585
C	0.93746	0.52096	0.41110
C	0.96900	0.53889	0.40559
C	0.98334	0.55957	0.20766
C	0.96543	0.56273	0.01846
C	0.93367	0.54479	0.02475
C	0.68399	0.31693	0.43874
C	0.65204	0.30261	0.43644
C	0.73555	0.36426	0.44599
C	0.75136	0.37559	0.21597
C	0.39430	0.59235	0.26423

C	0.39698	0.56624	0.26143
C	0.37155	0.53720	0.25625
C	0.34274	0.53461	0.25909
C	0.33985	0.56083	0.26179
C	0.36574	0.58999	0.26354
C	0.37610	0.51052	0.24275
C	0.41434	0.49421	0.18364
C	0.39759	0.46367	0.25729
C	0.41066	0.44497	0.24514
C	0.44060	0.45653	0.15929
C	0.45706	0.48719	0.08729
C	0.44401	0.50563	0.09934
C	0.68682	0.36597	0.43725
C	0.70170	0.34875	0.43862
C	0.63972	0.37016	0.42918
C	0.63020	0.37610	0.16063
C	0.40315	0.80189	0.26592
C	0.42965	0.83029	0.26536
C	0.45834	0.83303	0.26542
C	0.46017	0.80633	0.26981
C	0.43356	0.77761	0.26958
C	0.40477	0.77522	0.26710
C	0.48549	0.86387	0.25747
C	0.50328	0.91888	0.20596
C	0.53360	0.93161	0.28554
C	0.55298	0.96326	0.27971
C	0.54235	0.98261	0.19449
C	0.51190	0.96947	0.11640
C	0.49278	0.93808	0.12205
C	0.63748	0.31990	0.43480
C	0.65478	0.35167	0.43531
C	0.63417	0.26949	0.44092

C	0.62963	0.25422	0.20827
C	0.19268	0.60528	0.25537
C	0.16527	0.60541	0.25343
C	0.16466	0.63252	0.26134
C	0.19238	0.65995	0.27313
C	0.22005	0.65985	0.26975
C	0.22033	0.63232	0.26002
C	0.13488	0.63119	0.25930
C	0.08015	0.59919	0.16694
C	0.06752	0.60924	0.35439
C	0.03593	0.59709	0.36448
C	0.01680	0.57509	0.18574
C	0.02970	0.56550	0.99839
C	0.06100	0.57739	0.98992
C	0.31556	0.68271	0.98153
C	0.34744	0.69680	0.98257
C	0.26417	0.63578	0.98432
C	0.24867	0.62444	0.75192
C	0.60561	0.40763	0.65011
C	0.60287	0.43371	0.64786
C	0.62826	0.46278	0.65208
C	0.65710	0.46542	0.65813
C	0.66005	0.43923	0.65832
C	0.63421	0.41006	0.65374
C	0.62369	0.48947	0.65339
C	0.58525	0.50599	0.62493
C	0.60233	0.53607	0.71185
C	0.58919	0.55470	0.72268
C	0.55881	0.54353	0.64740
C	0.54203	0.51333	0.56123
C	0.55519	0.49497	0.55003
C	0.31179	0.63303	0.98103

C	0.29763	0.65086	0.98043
C	0.35876	0.62847	0.98792
C	0.36978	0.62394	0.75679
C	0.59708	0.19822	0.71353
C	0.57060	0.16980	0.71093
C	0.54190	0.16703	0.71164
C	0.54004	0.19371	0.71580
C	0.56663	0.22245	0.71632
C	0.59543	0.22487	0.71540
C	0.51475	0.13616	0.70854
C	0.49686	0.08096	0.67228
C	0.46680	0.06861	0.75406
C	0.44747	0.03695	0.75813
C	0.45790	0.01720	0.68105
C	0.48809	0.02997	0.60032
C	0.50715	0.06137	0.59587
C	0.36133	0.67881	0.98342
C	0.34360	0.64688	0.98202
C	0.36584	0.73028	0.98895
C	0.37054	0.74584	0.75740
C	0.80737	0.39461	0.73253
C	0.83476	0.39446	0.73688
C	0.83536	0.36736	0.72749
C	0.80765	0.33995	0.71147
C	0.77999	0.34008	0.71118
C	0.77970	0.36760	0.72351
C	0.86513	0.36866	0.73054
C	0.91982	0.40063	0.82478
C	0.93253	0.39070	0.63693
C	0.96413	0.40291	0.62718
C	0.98321	0.42484	0.80664
C	0.97023	0.43429	0.99447

C	0.93892	0.42234	0.00259
C	0.68625	0.31920	0.93886
C	0.65440	0.30400	0.93671
C	0.73635	0.36640	0.94586
C	0.75084	0.36830	0.71456
C	0.42546	0.63937	0.76458
C	0.44856	0.63159	0.75965
C	0.44099	0.60095	0.75513
C	0.41053	0.57872	0.76218
C	0.38752	0.58620	0.76424
C	0.39464	0.61658	0.76512
C	0.46284	0.59003	0.72279
C	0.51134	0.59395	0.71046
C	0.50625	0.57464	0.50155
C	0.52240	0.55924	0.47707
C	0.54413	0.56268	0.66120
C	0.55040	0.58339	0.86294
C	0.53425	0.59904	0.88569
C	0.68854	0.36844	0.93740
C	0.70323	0.35128	0.93884
C	0.64104	0.37144	0.92927
C	0.63674	0.38219	0.66100
C	0.35649	0.78724	0.76173
C	0.36504	0.81834	0.75739
C	0.39584	0.84076	0.75559
C	0.41747	0.83164	0.76448
C	0.40922	0.80092	0.76678
C	0.37867	0.77832	0.76485
C	0.40755	0.87371	0.72585
C	0.40519	0.91929	0.72315
C	0.42485	0.93368	0.51832
C	0.44099	0.96528	0.50048

C	0.43797	0.98346	0.68724
C	0.41691	0.96894	0.88442
C	0.40053	0.93710	0.90059
C	0.63986	0.32152	0.93496
C	0.65679	0.35364	0.93552
C	0.63600	0.27005	0.94102
C	0.62366	0.25485	0.70896
C	0.21046	0.56806	0.76074
C	0.18012	0.54392	0.75872
C	0.15606	0.55003	0.75168
C	0.16282	0.58015	0.75254
C	0.19280	0.60401	0.75589
C	0.21698	0.59846	0.75831
C	0.12360	0.52667	0.73166
C	0.08052	0.47705	0.77669
C	0.06253	0.47913	0.58173
C	0.03099	0.46117	0.58726
C	0.01667	0.44044	0.78496
C	0.03460	0.43729	0.97403
C	0.06636	0.45525	0.96769
H	0.30262	0.69425	0.48248
H	0.56853	0.33692	0.15509
H	0.52780	0.35053	0.14265
H	0.59572	0.44494	0.14570
H	0.63572	0.43175	0.15409
H	0.54601	0.43322	0.06382
H	0.50783	0.43047	0.79985
H	0.47928	0.45728	0.79645
H	0.43471	0.41175	0.49125
H	0.46356	0.38456	0.48903
H	0.30016	0.60825	0.48188
H	0.66756	0.23006	0.21467

H	0.65256	0.17529	0.20755
H	0.55896	0.15159	0.20958
H	0.57350	0.20517	0.21407
H	0.56919	0.11259	0.12948
H	0.57149	0.07759	0.85124
H	0.54331	0.02224	0.83716
H	0.58715	0.01961	0.53685
H	0.61579	0.07563	0.54480
H	0.38592	0.69164	0.48613
H	0.77117	0.43689	0.21828
H	0.82459	0.47937	0.23157
H	0.85521	0.41447	0.24165
H	0.80290	0.37293	0.22937
H	0.89168	0.46540	0.31759
H	0.92708	0.50494	0.56506
H	0.98226	0.53561	0.54975
H	0.97609	0.57843	0.86259
H	0.92010	0.54662	0.87373
H	0.69496	0.30336	0.44140
H	0.41458	0.61443	0.26453
H	0.41955	0.56919	0.26018
H	0.32262	0.51244	0.25535
H	0.31755	0.55851	0.26038
H	0.35701	0.48785	0.26161
H	0.37480	0.45441	0.32720
H	0.39731	0.42146	0.30111
H	0.48032	0.49719	0.02571
H	0.45711	0.52918	0.04407
H	0.70016	0.39050	0.43775
H	0.38137	0.80077	0.26323
H	0.42730	0.85031	0.26274
H	0.48204	0.80770	0.27011

H	0.43530	0.75726	0.26971
H	0.50786	0.86670	0.28009
H	0.54216	0.91734	0.35529
H	0.57630	0.97259	0.34017
H	0.50260	0.98349	0.05503
H	0.46941	0.92845	0.06215
H	0.61299	0.30875	0.43325
H	0.19227	0.58377	0.25175
H	0.14435	0.58386	0.24853
H	0.19259	0.68131	0.28072
H	0.24122	0.68113	0.27476
H	0.13296	0.65015	0.32986
H	0.08182	0.62515	0.49951
H	0.02633	0.60417	0.51515
H	0.01546	0.54763	0.86696
H	0.07050	0.56896	0.84961
H	0.30477	0.69645	0.98262
H	0.58536	0.38553	0.64920
H	0.58028	0.43072	0.64443
H	0.67720	0.48761	0.66247
H	0.68236	0.44159	0.66340
H	0.64282	0.51203	0.67932
H	0.62546	0.54501	0.77492
H	0.60281	0.57785	0.78869
H	0.51845	0.50359	0.50703
H	0.54184	0.47176	0.48463
H	0.29811	0.60852	0.98179
H	0.61888	0.19938	0.71236
H	0.57298	0.14980	0.70854
H	0.51815	0.19232	0.71660
H	0.56486	0.24278	0.71690
H	0.49244	0.13341	0.73137

H	0.45841	0.08320	0.81815
H	0.42435	0.02792	0.82014
H	0.49726	0.01568	0.54498
H	0.53034	0.07072	0.53429
H	0.38580	0.68960	0.98612
H	0.80780	0.41614	0.73539
H	0.85568	0.41600	0.74384
H	0.80743	0.31860	0.70168
H	0.75883	0.31883	0.69984
H	0.86710	0.34977	0.65880
H	0.91829	0.37486	0.49123
H	0.97379	0.39594	0.47619
H	0.98442	0.45209	0.12656
H	0.92936	0.43068	0.14325
H	0.69780	0.30619	0.94151
H	0.43148	0.66299	0.76371
H	0.47208	0.64921	0.75270
H	0.40398	0.55488	0.76006
H	0.36410	0.56822	0.76361
H	0.45326	0.56616	0.67596
H	0.48939	0.57128	0.35896
H	0.51769	0.54440	0.31421
H	0.56678	0.58646	0.00943
H	0.53841	0.61396	0.04681
H	0.70166	0.39298	0.93781
H	0.33275	0.77015	0.75892
H	0.34788	0.82494	0.74910
H	0.44141	0.84841	0.76465
H	0.42675	0.79480	0.76866
H	0.43140	0.88743	0.68002
H	0.42790	0.92027	0.37377
H	0.45608	0.97552	0.34078

H	0.41411	0.98215	0.03259
H	0.38535	0.92623	0.05851
H	0.61536	0.31017	0.93337
H	0.22880	0.56313	0.76223
H	0.17536	0.52068	0.75745
H	0.14482	0.58565	0.74965
H	0.19716	0.62717	0.75594
H	0.10821	0.53470	0.67869
H	0.07290	0.49518	0.42801
H	0.01772	0.46446	0.44328
H	0.02395	0.42157	0.12976
H	0.07995	0.45342	0.11853
N	0.50818	0.39356	0.17286
N	0.60853	0.11307	0.23204
N	0.88740	0.50174	0.19902
N	0.40330	0.51519	0.20206
N	0.48163	0.88703	0.21817
N	0.11136	0.60688	0.17075
N	0.59633	0.48496	0.62267
N	0.51852	0.11286	0.67600
N	0.88862	0.39291	0.82056
N	0.49198	0.60666	0.75425
N	0.39171	0.88704	0.76117
N	0.11261	0.49831	0.79301

630 **Supplementary Table 7.** Unit cell parameters and fractional atomic coordinates for
 631 CPOF-5-265 °C-84 h.

Space group		<i>P</i> 1	
Unit cell		$a = 58.3743 \text{ \AA}$, $b = 58.3390 \text{ \AA}$, $c = 5.3044 \text{ \AA}$, $\alpha = 89.9^\circ$, $\beta = 89.9^\circ$, $\gamma = 120.2^\circ$	
Pawley refinement		$R_p = 4.44\%$, $R_{wp} = 5.94\%$	
Atoms	x	y	z
C	0.35781	0.63374	0.45974
C	0.34588	0.6507	0.45462
C	0.36076	0.6238	0.22764
C	0.38873	0.6027	0.23518
C	0.39135	0.58016	0.23794
C	0.36899	0.55453	0.24258
C	0.34366	0.55179	0.23824
C	0.34089	0.5744	0.23384
C	0.36346	0.59999	0.23412
C	0.37267	0.53127	0.26045
C	0.43144	0.52638	0.40465
C	0.44183	0.50963	0.42858
C	0.42613	0.48246	0.37595
C	0.39971	0.47245	0.29931
C	0.38923	0.48935	0.27654
C	0.4052	0.51655	0.32921
C	0.43325	0.44634	0.20663
C	0.45557	0.46873	0.58812
C	0.43795	0.46517	0.39321
C	0.36211	0.67836	0.45463
C	0.36724	0.72316	0.45872
C	0.35054	0.69437	0.45424
C	0.37236	0.73642	0.22602
C	0.3612	0.77267	0.22858

C	0.36906	0.79977	0.22667
C	0.39616	0.81908	0.2287
C	0.415	0.81097	0.23124
C	0.40733	0.78409	0.23218
C	0.38035	0.76473	0.23137
C	0.40633	0.84783	0.22335
C	0.38741	0.89789	0.19969
C	0.39824	0.92542	0.17925
C	0.42453	0.94174	0.09669
C	0.43954	0.92992	0.03204
C	0.42873	0.9026	0.05167
C	0.40273	0.88631	0.14158
C	0.45476	0.98546	0.89085
C	0.43231	0.98502	0.27348
C	0.43685	0.97105	0.0841
C	0.32275	0.6829	0.45496
C	0.27712	0.64289	0.46067
C	0.30635	0.65521	0.45515
C	0.26353	0.63468	0.2291
C	0.22685	0.58721	0.23409
C	0.19968	0.56806	0.23261
C	0.18066	0.57609	0.23427
C	0.18912	0.6032	0.2359
C	0.21606	0.62232	0.23591
C	0.23514	0.61446	0.236
C	0.15186	0.55762	0.22929
C	0.10113	0.48854	0.20414
C	0.07359	0.47198	0.18281
C	0.05763	0.48223	0.09996
C	0.06981	0.50921	0.03616
C	0.09715	0.52559	0.0567
C	0.11307	0.51559	0.14668

C	0.01426	0.4691	0.892
C	0.014	0.44675	0.2747
C	0.02831	0.46537	0.086
C	0.31803	0.63914	0.45513
C	0.6422	0.36624	0.52106
C	0.65412	0.34928	0.52618
C	0.63501	0.37234	0.25328
C	0.58755	0.36118	0.25074
C	0.56839	0.36906	0.25269
C	0.57638	0.39617	0.25032
C	0.60347	0.41503	0.24748
C	0.6226	0.40734	0.24676
C	0.61478	0.38034	0.24763
C	0.55789	0.40635	0.25561
C	0.4888	0.38741	0.28118
C	0.4722	0.39824	0.30202
C	0.48237	0.42454	0.3839
C	0.50932	0.43958	0.44734
C	0.52574	0.42877	0.42731
C	0.51582	0.40275	0.33819
C	0.46913	0.45472	0.59029
C	0.4469	0.43234	0.20841
C	0.46547	0.43685	0.39711
C	0.63788	0.32162	0.52616
C	0.63275	0.27682	0.52205
C	0.64946	0.3056	0.52655
C	0.62385	0.26398	0.25405
C	0.60273	0.21474	0.24728
C	0.5802	0.18943	0.24509
C	0.55459	0.18602	0.24081
C	0.55187	0.20862	0.24491
C	0.57448	0.23414	0.24857

C	0.60005	0.23731	0.24777
C	0.53134	0.15892	0.22332
C	0.52643	0.0952	0.07876
C	0.50967	0.06795	0.05443
C	0.4825	0.05632	0.10702
C	0.47249	0.07268	0.18411
C	0.48941	0.10017	0.20722
C	0.5166	0.11155	0.1545
C	0.44633	0.01278	0.27581
C	0.46878	0.01312	0.89361
C	0.46519	0.0271	0.08917
C	0.67724	0.31706	0.52583
C	0.72286	0.35707	0.52012
C	0.69364	0.34475	0.52565
C	0.7361	0.36109	0.25243
C	0.78535	0.389	0.24317
C	0.8105	0.39157	0.24034
C	0.81354	0.36916	0.23686
C	0.79074	0.34384	0.24257
C	0.76539	0.34112	0.24725
C	0.76259	0.36374	0.24589
C	0.84047	0.37279	0.21915
C	0.90461	0.43149	0.07312
C	0.93181	0.44185	0.04998
C	0.94312	0.42613	0.10445
C	0.92646	0.3997	0.18201
C	0.89901	0.38925	0.20406
C	0.88797	0.40526	0.14967
C	0.98626	0.43314	0.27566
C	0.98662	0.45558	0.89332
C	0.9723	0.43792	0.0882
C	0.68197	0.36083	0.52568

C	0.35691	0.63294	0.95981
C	0.3446	0.64955	0.9547
C	0.36499	0.62764	0.72762
C	0.41245	0.63881	0.7359
C	0.43162	0.63095	0.74008
C	0.42363	0.60384	0.73999
C	0.39655	0.58497	0.73755
C	0.37741	0.59265	0.73527
C	0.38523	0.61964	0.73411
C	0.44212	0.59366	0.74694
C	0.51121	0.61259	0.77224
C	0.5278	0.60176	0.79435
C	0.51761	0.5755	0.87828
C	0.49065	0.56051	0.94248
C	0.47424	0.57132	0.92122
C	0.48418	0.59729	0.83003
C	0.53078	0.54538	0.0874
C	0.55311	0.56762	0.70435
C	0.5345	0.56318	0.89291
C	0.36063	0.67746	0.95421
C	0.36605	0.72287	0.95873
C	0.34905	0.69362	0.95419
C	0.37614	0.73599	0.72677
C	0.39725	0.78522	0.73198
C	0.41979	0.81054	0.73086
C	0.4454	0.81395	0.72748
C	0.44811	0.79134	0.7313
C	0.42551	0.76582	0.73356
C	0.39994	0.76266	0.73299
C	0.46867	0.84106	0.71126
C	0.4737	0.90491	0.56882
C	0.49047	0.93219	0.54695

C	0.51758	0.94379	0.60168
C	0.52751	0.92735	0.67829
C	0.51059	0.89983	0.69909
C	0.48346	0.88849	0.64438
C	0.55359	0.98709	0.77452
C	0.53146	0.98729	0.39251
C	0.53488	0.97304	0.58666
C	0.32132	0.68162	0.95498
C	0.27663	0.64166	0.96062
C	0.30537	0.65376	0.95515
C	0.2639	0.63887	0.7284
C	0.21464	0.61095	0.73609
C	0.18949	0.60837	0.73559
C	0.18644	0.63077	0.73135
C	0.20923	0.6561	0.73359
C	0.23459	0.65882	0.73485
C	0.2374	0.63621	0.73486
C	0.15949	0.62713	0.71525
C	0.09533	0.56838	0.57358
C	0.06814	0.55804	0.55056
C	0.05685	0.57381	0.60369
C	0.07352	0.60025	0.68002
C	0.10095	0.61067	0.70185
C	0.11198	0.59463	0.64859
C	0.01366	0.56681	0.77427
C	0.01346	0.54444	0.39238
C	0.02769	0.56206	0.58717
C	0.31693	0.63772	0.9556
C	0.64308	0.36702	0.021
C	0.65539	0.35042	0.0261
C	0.63923	0.37616	0.75313
C	0.61126	0.39726	0.74713

C	0.60863	0.4198	0.74765
C	0.631	0.44543	0.75064
C	0.65633	0.44817	0.7471
C	0.6591	0.42556	0.74562
C	0.63653	0.39997	0.7467
C	0.62731	0.4687	0.76642
C	0.56852	0.47364	0.90908
C	0.55812	0.4904	0.93123
C	0.57381	0.51754	0.8765
C	0.60025	0.52753	0.79955
C	0.61074	0.51062	0.77852
C	0.59476	0.48345	0.83329
C	0.56675	0.5536	0.70404
C	0.54433	0.53136	0.08669
C	0.56199	0.53484	0.89198
C	0.63936	0.3225	0.02658
C	0.63395	0.27709	0.02206
C	0.65095	0.30635	0.0266
C	0.62765	0.26355	0.75467
C	0.63883	0.22732	0.74634
C	0.63097	0.20022	0.74206
C	0.60388	0.18091	0.74248
C	0.58502	0.18901	0.74527
C	0.59269	0.21588	0.74735
C	0.61966	0.23525	0.74847
C	0.59371	0.15217	0.73544
C	0.61261	0.10209	0.70837
C	0.60178	0.07459	0.68575
C	0.57555	0.05838	0.60203
C	0.56059	0.0703	0.53864
C	0.57139	0.09759	0.5604
C	0.59734	0.11375	0.65131

C	0.54549	0.01496	0.39232
C	0.56762	0.01485	0.77471
C	0.56323	0.02909	0.58676
C	0.67868	0.31835	0.02581
C	0.72338	0.35833	0.02017
C	0.69462	0.34622	0.02564
C	0.73647	0.36529	0.75159
C	0.77314	0.41276	0.74086
C	0.80031	0.43191	0.73618
C	0.81933	0.42388	0.73694
C	0.81088	0.39678	0.7406
C	0.78394	0.37766	0.74362
C	0.76485	0.38552	0.74384
C	0.84813	0.44235	0.72956
C	0.89883	0.51145	0.70366
C	0.92637	0.52801	0.68189
C	0.94235	0.5178	0.59838
C	0.93016	0.49085	0.53406
C	0.90283	0.47447	0.55493
C	0.88689	0.48443	0.64589
C	0.98581	0.53095	0.39081
C	0.98591	0.55322	0.77314
C	0.97168	0.53465	0.58452
C	0.68306	0.36225	0.0252
N	0.39638	0.53531	0.30135
N	0.39166	0.85814	0.17221
N	0.14126	0.53255	0.17771
N	0.53282	0.39168	0.30742
N	0.53537	0.13926	0.18239
N	0.86033	0.39648	0.17715
N	0.46719	0.60836	0.79782
N	0.46467	0.86074	0.67047

N	0.13962	0.60342	0.67519
N	0.6036	0.46467	0.80723
N	0.6084	0.14189	0.68386
N	0.85871	0.46744	0.67814
H	0.40633	0.62218	0.23428
H	0.41121	0.58307	0.2392
H	0.3261	0.53228	0.24131
H	0.32126	0.57201	0.23138
H	0.35574	0.51143	0.24812
H	0.44413	0.54734	0.4409
H	0.46243	0.51814	0.48194
H	0.38716	0.45157	0.25776
H	0.36897	0.48115	0.21471
H	0.41998	0.44336	0.05275
H	0.45919	0.48269	0.73753
H	0.38352	0.68732	0.45582
H	0.34029	0.75791	0.22629
H	0.35413	0.80558	0.22362
H	0.43601	0.82551	0.22983
H	0.42236	0.77842	0.23249
H	0.42735	0.86055	0.25551
H	0.36723	0.88565	0.26545
H	0.38606	0.93391	0.22741
H	0.45994	0.94184	0.9711
H	0.44089	0.89433	0.9968
H	0.45825	0.97532	0.73884
H	0.41886	0.97453	0.42636
H	0.31398	0.69547	0.45642
H	0.24139	0.58088	0.23203
H	0.19361	0.54721	0.2302
H	0.17479	0.60984	0.23421
H	0.222	0.64314	0.23496

H	0.13937	0.56611	0.26156
H	0.1131	0.4804	0.26995
H	0.06481	0.45119	0.23041
H	0.05816	0.51789	0.97506
H	0.10571	0.54614	0.00233
H	0.02466	0.48282	0.74048
H	0.02423	0.44362	0.42809
H	0.30552	0.61771	0.45681
H	0.58125	0.34027	0.2533
H	0.54756	0.35412	0.256
H	0.61008	0.43604	0.24858
H	0.6434	0.42238	0.24645
H	0.56635	0.42739	0.22296
H	0.48072	0.36723	0.21604
H	0.45144	0.38605	0.25476
H	0.51794	0.45998	0.50771
H	0.54626	0.44094	0.48132
H	0.48281	0.4582	0.74179
H	0.44383	0.41892	0.05561
H	0.61648	0.31266	0.52497
H	0.62219	0.21672	0.24812
H	0.58309	0.17249	0.24398
H	0.53237	0.20655	0.24214
H	0.5721	0.25139	0.25088
H	0.51151	0.1559	0.23571
H	0.54739	0.10359	0.04246
H	0.51816	0.0559	0.00073
H	0.45161	0.06422	0.22568
H	0.48121	0.11218	0.2693
H	0.44332	0.02301	0.43014
H	0.48276	0.02361	0.74417
H	0.686	0.3045	0.52437

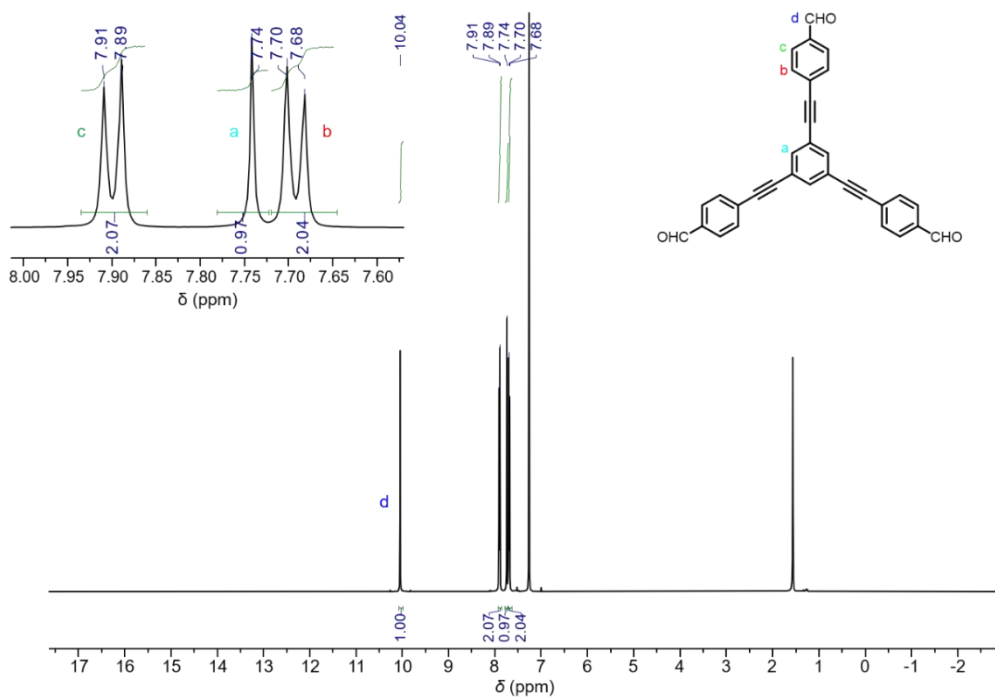
H	0.78365	0.40664	0.24298
H	0.8276	0.41142	0.23809
H	0.79253	0.32625	0.24045
H	0.74799	0.32149	0.25081
H	0.84322	0.35582	0.2328
H	0.89648	0.4442	0.03547
H	0.94409	0.46245	0.99586
H	0.93464	0.38712	0.22491
H	0.88677	0.369	0.26676
H	0.97578	0.41984	0.42957
H	0.97641	0.45926	0.74323
H	0.69449	0.38226	0.524
H	0.41875	0.65973	0.73462
H	0.45245	0.64589	0.74244
H	0.38994	0.56396	0.73988
H	0.35661	0.5776	0.73414
H	0.43366	0.5726	0.71628
H	0.51931	0.63275	0.70549
H	0.54857	0.61393	0.74646
H	0.48201	0.54013	0.00439
H	0.45372	0.55918	0.97593
H	0.51707	0.54197	0.23884
H	0.55623	0.58099	0.55059
H	0.38205	0.68656	0.95517
H	0.37779	0.78325	0.7305
H	0.41689	0.82748	0.72952
H	0.46761	0.79342	0.72859
H	0.42789	0.74857	0.73351
H	0.48848	0.84407	0.72487
H	0.45279	0.89653	0.53093
H	0.48201	0.94428	0.49355
H	0.54834	0.93576	0.72138

H	0.51872	0.88775	0.76105
H	0.55646	0.97665	0.92787
H	0.51761	0.97702	0.24212
H	0.31219	0.69386	0.95646
H	0.21634	0.59331	0.73563
H	0.17239	0.58851	0.73539
H	0.20744	0.67368	0.7302
H	0.25199	0.67846	0.73355
H	0.15675	0.6441	0.72779
H	0.10346	0.55565	0.53683
H	0.05585	0.53744	0.49743
H	0.06534	0.61285	0.72197
H	0.1132	0.63095	0.76338
H	0.02407	0.58008	0.92805
H	0.02373	0.54079	0.24259
H	0.30453	0.61629	0.95751
H	0.59365	0.37778	0.74868
H	0.58878	0.41689	0.74882
H	0.67388	0.46769	0.74951
H	0.67873	0.42795	0.74586
H	0.64424	0.48854	0.7527
H	0.55583	0.4527	0.94698
H	0.53751	0.48191	0.98489
H	0.6128	0.54838	0.75642
H	0.631	0.51879	0.71638
H	0.58005	0.55652	0.55027
H	0.54067	0.51746	0.23712
H	0.61794	0.3134	0.02563
H	0.65973	0.24208	0.74736
H	0.64591	0.19442	0.7394
H	0.56402	0.17447	0.74321
H	0.57765	0.22155	0.74849

H	0.57266	0.13943	0.76646
H	0.63273	0.11425	0.77491
H	0.61392	0.06603	0.73304
H	0.54024	0.05845	0.47694
H	0.55928	0.10593	0.50625
H	0.54212	0.02531	0.24131
H	0.58094	0.02513	0.9284
H	0.68782	0.30612	0.02433
H	0.7586	0.41909	0.74168
H	0.80638	0.45276	0.73292
H	0.82521	0.39014	0.73882
H	0.778	0.35684	0.74601
H	0.86063	0.43386	0.76063
H	0.88686	0.51956	0.77021
H	0.93514	0.54878	0.72981
H	0.94182	0.48219	0.47243
H	0.89427	0.45395	0.50022
H	0.97548	0.51728	0.23932
H	0.97563	0.55632	0.92636
H	0.69545	0.38369	0.0233

632

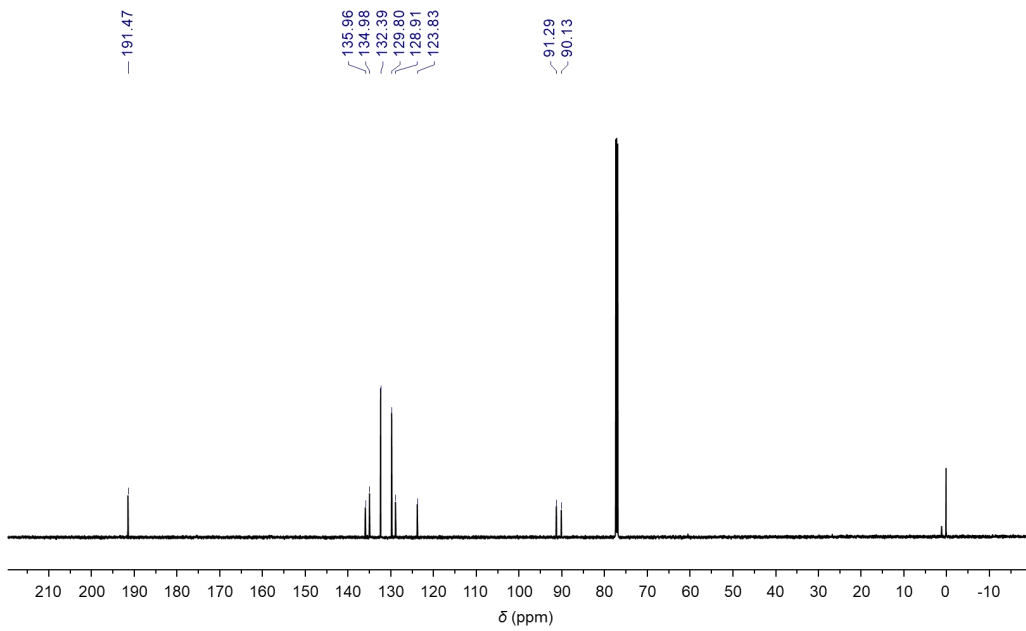
633



634

635 **Supplementary Figure 86.** The ^1H NMR spectra of
636 1,3,5-tri(4-formylphenylethynyl)benzene in CDCl_3 .

637



638

639 **Supplementary Figure 87.** The ^{13}C NMR spectra of
640 1,3,5-tri(4-formylphenylethynyl)benzene in CDCl_3 .

641

642 **Section S20. References**

- 643 [1] Perdew JP, Burke K, Ernzerhof M. Generalized gradient approximation made
644 simple. *Phys Rev Lett* 1996;77:3865. [DOI: [10.1103/PhysRevLett.77.3865](https://doi.org/10.1103/PhysRevLett.77.3865)]
- 645 [2] Kresse G, Furthmüller J. Efficiency of ab-initio total energy calculations for metals
646 and semiconductors using a plane-wave basis set. *Comput Mater Sci* 1996;6:15. [DOI:
647 [10.1016/0927-0256\(96\)00008-0](https://doi.org/10.1016/0927-0256(96)00008-0)]
- 648 [3] Kresse G, Furthmuller J. Efficient iterative schemes for ab initio total-energy
649 calculations using a plane-wave basis set. *Physical Review B Condensed Matter*
650 1996;54:11169. [DOI: [10.1103/PhysRevB.54.11169](https://doi.org/10.1103/PhysRevB.54.11169)]
- 651 [4] Yin ZJ, Xu SQ, Zhan TG, Qi QY, Wu ZQ, Zhao X. Ultrahigh volatile iodine uptake
652 by hollow microspheres formed from a heteropore covalent organic framework. *Chem*
653 *Commun* 2017;53:7266. [PMID: 28265612 DOI: [10.1039/c7cc01045a](https://doi.org/10.1039/c7cc01045a)]
- 654 [5] Wang P, Xu Q, Li Z, Jiang W, Jiang Q, Jiang D. Exceptional iodine capture in 2D
655 covalent organic frameworks. *Adv Mater* 2018;e1801991. [PMID: 29806216 DOI:
656 [10.1002/adma.201801991](https://doi.org/10.1002/adma.201801991)]
- 657 [6] Xing G, Zheng W, Gao L, et al. Nonplanar rhombus and kagome 2D covalent
658 organic frameworks from distorted aromatics for electrical conduction. *J Am Chem Soc*
659 2022;144:5042. [PMID: 35189061 DOI: [10.1021/jacs.1c13534](https://doi.org/10.1021/jacs.1c13534)]
- 660 [7] Li H, Chang J, Li S, et al. Three-dimensional tetrathiafulvalene-based covalent
661 organic frameworks for tunable electrical conductivity. *J Am Chem Soc*
662 2019;141:13324. [PMID: 31398976 DOI: [10.1021/jacs.9b06908](https://doi.org/10.1021/jacs.9b06908)]